Has CDMS seen one? Try XENON
Recent Progress on the Direct Detection of Dark Matter

Submitted by **Flip Tanedo**

on May 3, 2010 in partial fulfillment of the requirements for the advancement to candidacy for the degree of doctor of philosophy at Cornell University.

Institute for High Energy Phenomenology,
Newman Laboratory of Elementary Particle Physics,
Cornell University, Ithaca, NY 14853, USA

E-mail: pt267@cornell.edu

Prompt

In June of this year the XENON100 experiment will release its first results as the state-of-the-art search for dark matter via direct detection. This A Exam question reviews the principles of dark matter direct detection (focusing on liquid xenon techniques) and serves as preparation for the XENON100 results and their interpretation.

1. Review the kinematics of nuclear recoil as applicable to direct detection experiments and explain how this gives us the qualitative features of dark matter exclusion curves. Describe the astrophysical and theoretical assumptions that go into these curves. Review and interpret the latest exclusion plots.

2. Briefly review the major types of direct detection technologies and highlight the unique features of liquid xenon detectors. Explain in detail the XENON experimental set up: background elimination, sensitivity, and previous (XENON10) results. Discuss the expected sensitivity of XENON100.

3. Provide context for the upcoming XENON100 result by comparing the above discussion to suggestive dark matter results from complementary experiments such as DAMA (annual modulation). Identify broad classes of viable theoretical models.

4. Provide a 'road map' for future dark matter experiments and explain their interplay with one another and the Large Hadron Collider.

Contents

1 Introduction **1**

2 A historical introduction to dark matter **2**
2.1 'Dark Matter' Pre-History . . . 2
2.2 The Dark Matter Dark Ages . . . 2
2.3 The Dark Matter Renaissance . . . 3
2.4 Romanticist Dark Matter . . . 4
2.5 Baroque Dark Matter . . . 5
2.6 Impressionist Dark Matter . . . 6
2.7 Postmodern Dark Matter: looking forward . . . 7

3 Direct Detection: Theory **8**
3.1 General strategy . . . 9
3.2 Astrophysical input . . . 10
3.3 Phenomenological cross section . . . 11
3.4 Differential recoil rate, a first pass . . . 12
3.5 Comparing apples to apples . . . 16
3.6 More realistic velocities . . . 17
3.7 Form factor suppression: coherence lost . . . 19
3.8 Further refinement . . . 21

4 Direct Detection: Experiments **23**
4.1 Backgrounds . . . 24
4.2 Heat and charge . . . 24
4.3 Heat and light . . . 25
4.4 Light and charge . . . 26

5 The XENON experiment **26**
5.1 Xenon: what's inside XENON . . . 27
5.2 Light and Charge: Ionization and Scintillation . . . 28
5.3 Two-Phase Time Projection Chamber . . . 30
5.4 Calibration and background . . . 31
5.5 XENON10 . . . 33

6 Anticipating XENON 100 **34**
6.1 Reach of the XENON100 experiment . . . 36
6.2 What did CDMS see? . . . 36
6.3 CoGeNT, DAMA, CRESST . . . 36
6.4 Hints from Pamela/FERMI . . . 38
6.5 Role of the LHC . . . 39

7 Outlook **40**

A Notation and Conventions **41**

B Zero momentum transfer cross section **41**

C Review of Dark Matter tools **41**

D The WIMP miracle **42**

1 Introduction

One of the most significant scientific developments of the 20th century was the discovery—through multiple independent observations—that most of the matter in the universe is composed of a yet-unknown particle species which we call dark matter (DM). A confluence of astrophysical and cosmological experiments present an overwhelming case for the existence of a non-baryonic dark matter particle. Further, the relic density of such a particle is suggestive of a weakly interacting massive particle (WIMP) with a mass on the order of hundreds of GeV—precisely the scale at which we expect to see new physics at the Large Hadron Collider (LHC). This so-called 'WIMP miracle' ties together 'traditional' high energy physics with experiments conducted deep underground (direct detection) and high into the heavens (indirect detection). It is one of the most exciting directions in the search for new physics and is one of the mysteries of fundamental science that may plausibly be solved within our lifetimes. In fact, as we will discuss below, this is a particularly prescient time to review dark mater phenomenology since hints from cosmic ray and direct detection experiments may suggest a potential for new discoveries in the near future[1].

In this A Exam we review recent progress in the direct detection of dark matter, focusing on the XENON100 experiment and its immediate experimental and theoretical progress. We shall assume a working background in the broad ideas related to dark matter particle physics and will not attempt to adequately review materials available in standard textbooks; appropriately concise introductions can be found in [1]. A popular introduction can be found in [2]. We will attempt to provide as many references as possible to assist those who intend to do pursue future work in this field (such as the author). Our goal will be to provide a working guide for phenomenologists to interpret the XENON100 results to be released this summer. In so doing, we will review broadly applicable general aspects of direct detection phenomenology. The primary review literature for dark matter include [3, 4]. Reviews for the direct detection that will be the main focus of this report can be found in [5, 6, 7, 8, 9]. We will only provide cursory discussions of dark matter astrophysics/cosmology [10, 11, 12], collider searches [13], and model-building [14, 15, 16, 17, 18]. Additional websites which aggregate review literature and are regularly updated can be found in [19].

We begin in Section 2 with a historical introduction to dark matter in which we broadly discuss the status of the field and how it came to be. We feel that this is a particularly meaningful way to survey and relate the broad range of experimental and theoretical directions currently being pursued. In Section 3 we derive the relevant formulae for elastic scattering of WIMPs against nuclei. This will provide a quantitative foundation to understand the exclusion diagrams generated by direct detection experiments. In Section 4 we briefly discuss various types of direct detection methods and experiments, leading up to Section 5 where we present the XENON experiment. Section 6 highlights some aspects phenomenological context that has led to recent excitement in dark matter experiments. We conclude in 7 with an apology for how little we cover over so many pages. Appendix A explains our conventions while Appendix C highlights publicly available computer tools for dark matter phenomenology (aimed at theorists). Finally, Appendix D presents the so-called 'WIMP-miracle' of why one might expect dark matter particles 'right around the corner' in direct detection experiments and the LHC.

Other than its reasonably clever title, this document contains no original research. It is the

[1] Given recent delays and funding cuts, a better term phrase may be 'the *asymptotically* near future.'

hope of the author that it will be useful to other researchers as a review at this timely moment in the history of dark matter.

2 A historical introduction to dark matter

We begin with a selective history of dark matter highlighting some motivation and leading up to a subjective description of recent experimental and theoretical developments in the field. A more encyclopedic history can be found in [20]. We attempt to provide relevant references to assist those—such as the author—who intend to continue in this field.

2.1 'Dark Matter' Pre-History

The big question for dark matter experimentalists is how should we detect 'stuff' that isn't observable in the conventional sense. It is well known that dark matter was originally discovered through its gravitational effects, but the idea that non-luminous astronomical objects could be detected in this way is actually much older. Two of the earliest examples (from [21]) include (i) the discovery of white dwarfs due to the position of the stars Sirius and Procyon, and (ii) the discovery of Neptune from an anomalous orbit perturbation in Uranus.

2.2 The Dark Matter Dark Ages

An early history of dark matter with original references is presented in [22]. We will only briefly and selectively mention parts of this story. Dark matter was first proposed in 1933 by Fritz Zwicky to account for the radial velocity dispersion of galaxies in the Coma cluster [23] (English reprint [24]) which were suggestive of the presence of non-luminous matter. Zwicky's phrase '*dunkle (kalte) Materie*' is regarded as the origin of the term (cold, i.e. non-relativistic) dark matter. Zwicky's observations were later seen in the Virgo cluster [25] and later in the local group [26]. There is a rather famous photograph of Zwicky making a silly face (originally taken as part of a series of deliberately exaggerated expressions [27]) that now seems to be a *de facto* requirement for any public talk on dark matter.

At around the same time another set of astrophysical observations would lead to the 'classic' evidence for dark matter which undergrads will recite in some Pavlovian manner: the rotational velocity curves of spiral galaxies. Astronomers found that the outer regions of galaxies were rotating with unexpectedly high velocities given what was expected of their matter distribution based on luminous matter. The first such observations came in 1939 from the Andromeda galaxy [28] and were later extended in the to larger radii in the 1970s; see [29] for a history and references.

It is worth noting that papers on the 'missing mass' in galaxy clusters and that in the outer regions of spiral galaxies did not make connections between the two. These were also the dark ages of scientific publication, well before the arXiv. At this point these astrophysical results were, "at best, received with skepticism in many colloquia and meeting presentations" [22]. It is not necessarily comforting to remark that our scientific society has advanced so much that some of us are no longer burdened by such skepticism against experimental results [30].

A turning point came in 1973 with the work of Ostriker and Peebles that showed that instabilities in models of galaxy disks could be solved by a massive spherical component, a so-called

halo [31]. (Such a halo is a generic prediction of collision-less dark matter [32].) Further, with Yahil they noted that galaxy masses appear to increase linearly with radius [33]. These results, combined with the latest velocity curves at the time, provided a strong case for the existence of 'missing mass' in galaxies.

2.3 The Dark Matter Renaissance

Following this there were a Renaissance of astrophysical results which confirmed (in the scientific sense) and refined the missing mass hypothesis while ruling out known reasonable alternatives. These are reviewed nicely in Blitz's lectures in [4] and Gaitskell's lectures in [34]. An undergraduate-level discussion with calculations can be found in [35]. In addition to refined astrophysical searches of the general type discussed above[2] that rely on the virial theorem and hydrostatic equilibrium (reviwed in [37]), the 1990s brought about new astrophysical and cosmological methods to probe the nature of this 'missing mass' (see reviews in [10, 38]).

The detection of X-rays from hot gas in elliptical galaxies provided a new confirmation of the dark matter hypothesis. This provides a handle to determine the luminous matter content of the galaxy which one can compare to the matter required to maintain hydrostatic equilibrium. Fabricant et al. found that the total mass of the M87 galaxy is indeed ten times larger than the luminous mass [39]. While this was effectively the same type of analysis as the aforementioned 'dark age' experiments, this was convincing evidence that the 'missing mass' phenomenon was not exclusive to spiral galaxies.

Another clear observation of dark matter comes from the prediction of gravitational lensing in general relativity, reviewed in [40]. Here one observes the dark matter's presence by the way it gravitationally warps space and changes the path of light as it comes between luminous astrophysical objects and our telescopes. The effect can be seen at different magnitudes depending on the gravitational potential of the lensing object. Strong lensing refers to easily visible distortions of an individual light source. Weak lensing, on the other hand, requires a statistical analysis of a large number of sources to search for coherent distortions. Finally, microlensing comes from relatively light lensing objects whose distortions of the luminous object cannot be resolved so that one instead searches for a change in that objects overall luminosity. The most advanced lensing analyses have not only detected dark matter, but have even allowed astrophysicists to construct three dimensional maps of its distribution [40].

The previous two methods (X-ray spectroscopy and gravitational lensing) converged with the relatively recent observation of the Bullet cluster which was formed by the collision of two large galaxy clusters [41]. By using X-ray spectroscopy to image the hot (luminous) matter and weak gravitational lensing to image mass density, it was seen that the luminous matter lags behind the total mass as one would expect from weakly-interacting dark matter. This observation effectively put the nail in the coffin of dark matter alternative theories, such as modified Newtonian gravity.

The cosmic microwave background (CMB) has lifted cosmology out of its status as a largely-theoretical discipline[3]. A combination of theoretical and experimental cosmological constraints

[2] We will not discuss these further. One of the important lessons in the emerging field of particle astrophysics is that particle physicists should take astrophysical anomalies with a grain of salt, e.g. [36]. We will return to a modern manifestation of this in Section 2.5.

[3] As Shamit Kachru once remarked, "Until very recently, string cosmology was the marriage of a field with no

have cemented the so-called 'concordance' or ΛCDM (dark energy with cold dark matter) paradigm as an accurate description of our universe [35, 43]. The general strategy here is to measure the matter density of the universe $\Omega_m \approx 0.04$ and compare to the baryonic energy density $\Omega_b \approx 0.26$ of the universe and conclude that most of the matter in the universe must be composed of non-baryonic dark matter. Indirect measurements of Ω_b include analyses of primordial nucleosynthesis of ^{4}He, ^{2}H and ^{7}Li [44]; the Sunyaev Zel'dovich effect in which the spectrum of X-ray emission from hot gasses is shifted from inverse scattering off the CMB [45], and the Lyman-α forest whose absorption lines indicate the make up of the intergalactic medium [46]. The highlight of observational cosmology, however, was the direct measurement of the CMB spectrum from the COBE [47] and WMAP [48] satellites. The measurement of the acoustic peaks in this spectrum provide the most stringent constraints on dark matter (and dark energy) [49].

Further evidence comes from the requirement of dark matter in cosmology to generate the density perturbations that led to large scale structure [50] and to account for big bang nucleosynthesis [51].

2.4 Romanticist Dark Matter

While we have been necessarily brief and incomplete, it should be clear that the ΛCDM model with weakly-interacting cold dark matter has been well-established by a variety of astrophysical observations using orthogonal techniques and taken at a range of scales (galactic, galaxy cluster, and cosmological). What is remarkable is that at roughly the same time that the need for dark matter was becoming accepted dogma in astrophysics and cosmology, realistic theories of particle physics beyond the standard model also generically began to predict the existence of new stable massive states that were natural dark matter candidates. Thus the forefront of cosmology and astrophysics converged with particle physics and gave rise to particle-astrophysics (or astro-particle physics).

The theory community's favorite candidate for new fundamental physics is supersymmetry[4] (SUSY). Constraints on $B-L$ violation (proton decay) tend to set very restrictive bounds on new physics—often pushing them into an unnatural regime—unless some sort of parity is imposed to prevent dangerous higher-dimensional operators. In SUSY the standard solution is to impose R-parity, which makes the lightest supersymmetric partner (LSP) stable and a benchmark candidate for weakly-interacting massive particle (WIMP) dark matter.

The theory-side highlight of the dark matter Renaissance is the **Boltzmann equation**, whose integral determines the relic abundance of a thermally-produced WIMP particle species of known interaction cross section after the universe cools and the particle 'freezes out' of thermal equilibrium. This is the key to connect particle physics data (interaction cross section) with astrophysical data (relic density). This is the first tool for any honest theorist interested in dark matter and is discussed in classic (particle-)cosmology texts [11, 52]; also see [53] for a slightly more advanced analysis. Honestly integrating the Boltzmann equation is a notorious pain in the ass for generic models due to threshold effects and potential numerical instabilities. Fortunately, numerical tools now exist [54, 55] which we briefly mention in Appendix C. Non-thermal models (e.g.

data with a field with no predictions" [42].

[4]Given the overabundance of excellent references for SUSY, we will not mention any in particular.

non-thermal axions) are significantly more complicated but—due to kinetic equilibrium—tend to also contribute to thermal dark matter [56]; for constraints see, e.g. [57].

As reviewed in [17, 58], there are a number of viable dark matter candidates that go beyond the standard WIMP paradigm. These include sterile neutrinos, axions, and more recently explored exotica that we will mention in Section 2.7. (Other non-particle candidates, such as massive compact halo objects—MACHOs, have been shown to be unable to account for most of the dark matter mass.) However, there is a compelling coincidence called the **WIMP miracle** that has made WIMP models a favorite dark matter candidate among theorists [59]. If one assumes only that the dark matter couplings are on the order of those for the weak interaction ($g \approx 0.65$), then cranking through the Boltzmann equation gives a model-independent statement that the dark matter mass should be on the order of 100 GeV to 1 TeV; see Appendix D. This happens to be *precisely* where particle physicists already expect to find new physics to solve the hierarchy problem and illuminate the mechanism of electroweak symmetry breaking.

Since this brings us to the current era, let us review what is is 'known' about dark matter [15]:

1. It explains observations over a wide range of scales and experimental methodologies. In particular, it allows $\Omega_M h^2 \approx 0.1$ as required by cosmological observations.
2. It is neutral. This is strongly constrained by, for example, searches for heavy hydrogen [60]. (Millicharged DM is constrained by cosmology [61].)
3. It is not made up of Standard Model particles but is stable on Hubble time scales.
4. It is *cold*, i.e. non-relativistic at freeze-out ($T \sim$ keV), or else structure formation would fail.
5. It is effectively non-(self-)interacting due to the stability of the halo. (A more conservative statement is that DM must have negligible annihilation and dissipation, see e.g. [62].)
6. If DM interacts with a massless vector[5], then the coupling $\alpha \lesssim 10^{-3}$ for $m_\chi \sim$ TeV [63].
7. It violates the equivalence principle [64].

A similar 'ten point test' with further discussion can be found in [65].

2.5 Baroque Dark Matter

> *Particle physicists* also saw the dramatic style of Baroque *laboratory experiments* as a means of impressing visitors and expressing triumphant power and control [66] (modified by the author, who is aware that the Baroque period predated Romanticism).

The current era has particle physicists attempting to pull dark matter out of the sky and into the lab, where one might hope to directly measure dark matter scattering events against detector material. This so-called **direct detection** benefits from being largely independent of astrophysical uncertainties and unknowns (astrophysical assumptions will be explained in Section 3.2). These experiments are placed deep underground to shield against cosmic ray backgrounds and make use of state-of-the art techniques to determine the dark matter cross section and mass. The heuristic picture of direct detection is as follows:

[5] This restriction is not as random as it seems. Our favorite DM benchmark is the neutralino which is a Majorana fermion so that any interaction with gauge vectors would violate gauge invariance. The restriction that *generic* DM should have very small gauge vector couplings means that the neutralino is still a valid benchmark [15].

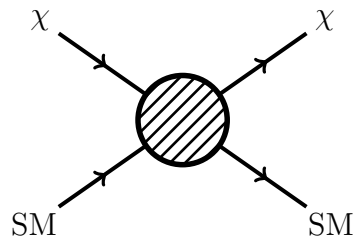

A WIMP from the local dark matter halo interacts with a target nucleus (composed of Standard Model quarks) in a detector and recoils. By counting the number of nuclear recoils, one can hope to determine information about the dark matter mass and cross section. The review of direct detection via liquid noble gas detectors is the main focus of this report so we shall leave further discussion of this topic to the rest of this document.

It is important to note that while exclusions plots continue to chip away at the allowed region (under standard assumptions), to date there has been no universally-accepted 'smoking gun signal' for dark matter via these techniques. A single experiment, the DAMA collaboration [67], has a many-standard deviation result. While the DAMA signal observes an annual modulation with the correct phase that one would expect from the motion of the Earth relative to the galactic dark matter halo, it has been effectively ruled out within the standard WIMP paradigm by, for example, the CDMS collaboration [68, 69, 70]. Additionally, DAMA's rudimentary background rejection and its exclusive contract with the company producing its NaI detector material have added to particle physics community's skepticism of their result; for an informal review see [71], or see [6] (lecture three) for a discussion of potential background sources. In fact, until recently these results were largely ignored by dark matter model-builders.

2.6 Impressionist Dark Matter

While a generation of particle physicists turned to direct detection to "pull dark matter from the sky and into the lab," astrophysicists had turned to **indirect detection** techniques to go back to the sky to search for dark matter annihilation, which is very nicely reviewed in [72]. The heuristic picture is

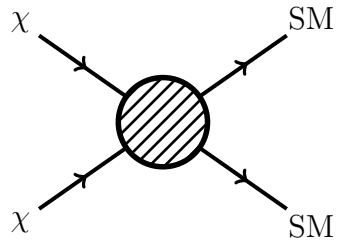

Here one hopes to detect the Standard Model products (or the products thereof) of dark matter annihilation in the halo. Smoking gun signatures include antimatter (positrons and anti-protons), gamma rays (mono-energetic), and neutrinos. These signals are affected by astrophysics, including hitherto unknown but otherwise boring astrophysics such as the possible existence of nearby pulsars that could mimic the above signals.

Several such intriguing astrophysical signals have existed for some time, but interest peaked rapidly in 2008 with the release of the positron and anti-proton flux data from the PAMELA satellite[6] [74]. PAMELA is particularly interesting because it is a 'toy' particle detector in space with its own magnetic field to determine particle charge (and hence discriminate between particles and anti-particles). The satellite found an unexpected increase in the charged lepton flux and a corresponding increase in the positron fraction[7] [76] with no similar feature in anti-protons [77]. More recently the Fermi Large Area Telescope [78] does not rule out PAMELA.

Astrophysicists were cautious to herald the PAMELA signal as an avatar of dark matter; see, e.g., [79] for two early alternate astrophysical explanations. On the other hand, having been starved of any data vaguely resembling new physics for some time, the particle theory community was quick to build new models [80] selectively invoking astrophysical hints. Other signals include HESS [81], INTEGRAL [82], EGRET [83], and the Fermi/WMAP "haze" (see [84] for a recent critical discussion) [85]. ATIC, a balloon experiment commonly cited in dark matter literature between 2008 and 2009, seems to have been ruled out by Fermi [78]. A general feature of these anomalies is that they seem to suggest dark matter with unusual spectra and/or couplings—though these are not necessarily consistent with one another.

2.7 Postmodern Dark Matter: looking forward

> Like all tyrannies, there is a single yoke of control: the one thing we know about WIMPs is their relic abundance. We've lived with this tyranny for a long time. It's provided all of us with jobs... and some of us with tenure.
> – Neal Weiner, on the 'tyranny' of the WIMP Miracle paradigm [86].

The prospect that astronomers had already indirectly detected dark matter beyond the standard neutralino-like paradigm spurred much interest in more exotic 'phenomenological' dark matter models that were motivated primarily from astrophysical anomalies rather than models of electroweak symmetry breaking. Key ideas include light dark matter [82, 87], inelastic dark matter [88, 89], annihilating dark matter [90], exothermic dark matter [91], superWIMPs [92] and WIMP-less dark matter [93]. (Additionally, some older top-down ideas have stuck around, e.g. axions [94].)

A watershed paper by Arkani-Hamed and Weiner [95] (using many ideas earlier proposed by the latter) established new rules for dark matter model building: pick your favorite anomalies (direct or indirect) and construct a model that explains them and makes some unique dark matter signature at colliders. The particle physics community, sitting on its thumbs while delays to the Large Hadron Collider (LHC) dampened their expectations of when to expect signals of new physics, was eager to pick up the trend. Thus came a renewed emphasis on direct production (collider signatures) of dark matter:

[6] Actually, interest in dark matter interpretations began well before data was officially released. One particularly bold collaboration published a paper based on a photograph preliminary results presented at a conference and even had the audacity to reproduce the preliminary results well before the official results were released [73].

[7] HEAT found a similar anomaly in the positron flux before PAMELA but could not rule our secondary sources [75]; we thank Bibhushan Shakya for this comment.

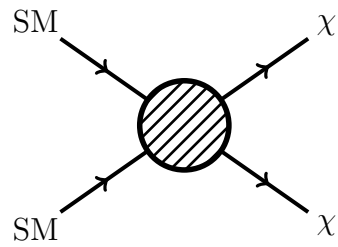

Note that this is just related by crossing symmetry to our picture of indirect detection. Thus even for 'phenomenological' models with arbitrary couplings and sectors, one would necessarily expect there to be some collider given sufficient luminosity and energy.

One effect of this resurgence was the cautious re-admittance of DAMA into the group of viable dark matter hints. While other direct detection experiments had seemed to rule out DAMA assuming a neutralino-like WIMP, these new models had various ways to be simultaneously consistent with the DAMA annual modulation and the other direct detection constraints [96]. As will be discussed below, one easy way to do this is to have dark matter with predominantly spin-dependent coupling [97] since DAMA's NaI detector material is notably more sensitive to such couplings compared to the Si and Ge targets used for the other existing direct detection bounds. An additional handle comes from including channelling and blocking effects [98] in DAMA [99] (these effects seem to only be particularly relevant for DAMA's NaI crystals and do not affect other existing direct detection experiments).

Finally, the most recent hints for dark matter come from the CDMS and CoGeNT collaborations. In December of 2009, CDMS announced two events that they could not rule out as dark matter hits [69]; see also [68] for recorded seminars announcing this result. While this is nowhere near a 'discovery,' optimists hope that this is a harbinger of actual events in the next generation of direct detection experiments (some of which are the subject of the rest of this exam). Finally, just a two months before the preparation of this document, the CoGeNT collaboration released a similar 'hint' that could be interpreted as a dark matter event [100, 101]. It is perhaps interesting to note that while the CoGeNT and DAMA signal regions appear mutually exclusive, invoking the channeling effects of the previous paragraph appears to give enough of a handle to allow the two regions to overlap outside of the region that is otherwise excluded by direct detection.

To close, we remark that a proper experimental understanding of dark matter can only come from combined results from all three methods of detection (direct, indirect, and collider); each method is complementary in that each depends on a different source of unknown input. These are summarized in Fig. 1a.

3 Direct Detection: Theory

After the above long-winded historical introduction, we now discuss general features of direct dark matter detection. Direct detection first demonstrated by Goodman and Witten (yes, *that* Witten) at around the time when the author was born [102]. As explained in the introduction, we study the scattering of halo dark matter particles off of highly-shielded targets to determine information about their interactions (cross sections) and kinematics (mass). Because dark matter is so weakly interacting with the Standard Model such experiments require large detector volumes,

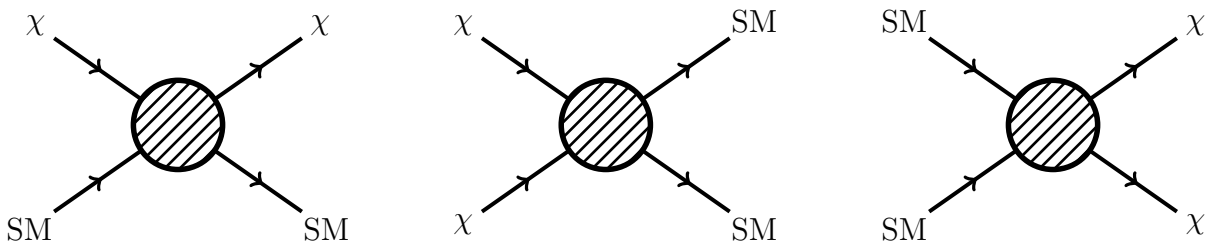

(a) Direct detection (b) Indirect detection (c) Collider production

Figure 1: Unknowns in dark matter experiments. (1a) What are the quark couplings? (1b) What are the final states? (1c) What are the parent species? This should be compared to the three wise monkeys: See no evil, hear no evil, speak no evil.

as is the case with neutrino experiments. Unlike neutrino experiments, however, dark matter is heavy and the detection methods are rather different. While neutrinos may zip through a liquid detector relativistically and leave easy-to-detect Čerenkov radiation, WIMPs lumber along like giant elephants that will absent-mindedly bump into target nuclei[8]. One can intuitively appreciate that the two scenarios very different kinematics that require separate detection techniques.

The canonical review of the calculation of dark matter direct detection constraints is reviewed exceptionally well by Lewin and Smith [103]. We shall review these results following the pedagogical discussion in [6]. Additional comments and applications to the CDMS detector are presented in chapter 2 of [70]. The key result will be to understand the structure of dark matter exclusion plots. We will also briefly survey and classify the experimental techniques used in the range of direct detection experiments to help place our specific study of XENON100 into proper context.

3.1 General strategy

A garden-variety neutralino-like WIMP interacts with a target material primarily through elastic collisions with the target nuclei. Experiments can then use complementary detection techniques to detect and distinguish such interactions from background events to compare to theoretical predictions. These theoretical predictions can be parameterized by the dark matter mass and a single effective coupling for typical WIMPs or up to four effective couplings for more general dark matter models depending on, e.g., spin coupling. The primary quantity to connect experimental data to theoretical models is the elastic nuclear recoil spectrum, dR/dE_R, where R is the recoil event rate and E_R is the energy of the recoiling nucleus.

We will start by assembling some pieces required to construct the recoil spectrum: the astrophysical input data about the WIMP velocity distribution and the effective ('phenomenological') cross section. Since we will see that most events occur with low recoil energy, it will be advantageous to further parameterize the cross section in terms of a zero momentum transfer part and a **form factor** that encodes the momentum and target dependence. In doing so we will uncover important general features that feed into the design of direct detection experiments.

[8]This behavior is very reminiscent of certain graduate students who shouldn't be trusted with delicate things.

3.2 Astrophysical input

Our primary astrophysical assumption is that the dark matter in the halo has a 'sufficiently' Maxwellian velocity distribution. The **Maxwell-Boltzmann distribution** describes the velocities of particles which move freely up to short collisions and is derived in one's favorite statistical physics textbook. Here one assumes that the WIMPs are isothermal and isotropically distributed in phase space (i.e. gravitationally relaxed). It is important to remark that this is not actually fully accurate and thus that WIMPs cannot have an *exactly* Maxwellian distribution even though such an approximation should be sufficient (i.e. with uncertainties smaller than those coming from the WIMP-nucleus cross section) for garden-variety WIMP models. For a recent discussion of the implications of the expected departures from the Maxwell distribution at the large velocity tail and the kinds of models that would be affected by this, see [104].

The complete phase space distribution for such a halo for a dark matter species of mass m_χ, gravitational potential $\Phi(\vec{x})$, and velocity in the galaxy frame $\vec{v}_{\rm gal}$ is

$$f(\vec{x},\vec{v})\, d^3x\, d^3v \propto \exp\left(-\frac{m_\chi\left[v^2/2+\Phi(\vec{x})\right]}{k_B T}\right). \tag{3.1}$$

The Earth is effectively at a fixed point in the gravitational potential so that the position dependence is is also fixed and can be absorbed into the overall normalization. We may thus write

$$f(v_{\rm gal}) = \frac{1}{k_0} e^{v_{\rm gal}^2/v_0^2} \tag{3.2}$$

where k is a factor to normalize the distribution

$$k_0 = \int d^3\vec{v}_{\rm gal}\, e^{v_{\rm gal}^2/v_0^2} = (\pi v_0^2)^{3/2} \tag{3.3}$$

and v_0 is the most probable WIMP speed and is given by the characteristic kinetic energy:

$$\frac{1}{2} m_\chi v_0^2 = k_B T \qquad\qquad v_0 \approx 220 \text{ km/s} \approx 0.75 \cdot 10^{-3}\, c. \tag{3.4}$$

Note that in (3.3) we have not defined the region of integration in velocity space, we will discuss this shortly. For now one can assume that we are integrating over the entire space. It is typically to write the $\vec{v}_{\rm gal}$ explicitly in terms of the velocity in the Earth (lab) frame, $\vec{v}$, and the velocity of this frame relative to the dark matter halo, $\vec{v}_E$,

$$\vec{v}_{\rm gal} = \vec{v} + \vec{v}_E. \tag{3.5}$$

The orbit of the Earth about the sun in the galactic halo frame provides the input for an annual modulation:

$$v_E = 232 + 15\, \cos\left(2\pi \frac{t - 152.5 \text{ days}}{365.25 \text{ days}}\right) \text{ km s}^{-1}. \tag{3.6}$$

All astrophysical data in this section come from [70]. Further discussion this data can be found in, e.g., [105].

A key observation on the right-hand side of (3.4) is that the dark matter particle is very non-relativistic (we include an explicitly factor of $c = 1$). This will have important implications on our WIMP-nucleon cross section.

Let us remark once again that for the remainder of this document (except for isolated remarks), we will *assume* this astrophysical input. While we have mentioned in Section 2.7 that there are many new phenomenological dark matter models that can deviate from these assumptions, we will not consider them in our primary analysis[9].

3.3 Phenomenological cross section

Given a matrix element $\mathcal{M}(q)$ for the scattering of WIMPs of lab frame velocity $\vec{v}$ against target nuclei with characteristic momentum transfer q, we may use Fermi's Golden Rule to determine the differential WIMP-nucleus cross section,

$$\frac{d\sigma_N(q)}{dq^2} = \frac{1}{\pi v^2} |\mathcal{M}|^2 = \hat{\sigma}_N \cdot \frac{F^2(q)}{4m_r^2 v^2}. \tag{3.7}$$

The $(\pi v^2)^{-1}$ factor comes from the density of final states and the usual 2π in the Golden Rule formula. In the last equality we've written the cross section in terms of a q-independent factor $\hat{\sigma}_N = \sigma_N(q = 0)$ and fit all of the momentum dependence into the remaining **form factor**, $F(q)$. We have written m_r for the reduced mass of the WIMP-nucleus system,

$$m_r = \frac{m_\chi m_N}{m_\chi + m_N}. \tag{3.8}$$

For a general interaction Lagrangian between WIMPs and nucleons, one can show that the $q = 0$ cross section can be parameterized by four effective couplings $f_{p,n}$ and $a_{p,n}$ (subscripts refer to proton and neutron couplings) according to

$$\hat{\sigma}_N = \frac{4m_r^2}{\pi} \left[Zf_p + (A - Z)f_n\right]^2 + \frac{32G_F^2 m_r^2}{\pi} \frac{(J+1)}{J} \left[a_p\langle S_p\rangle + a_n\langle S_n\rangle\right] \tag{3.9}$$

where J is the nuclear spin, Z (A) is the atomic (mass) number, and $S_{p,n}$ are the spin content of the proton and neutron [106]. There is an implied sum over nucleons, p and n. We have separated the zero momentum transfer cross section into **spin independent** (SI) and **spin-dependent** (SD) pieces. We elucidate the derivation of this paramterization in Appendix B. The relevant point is that this is still a general formula for the effective, zero momentum transfer cross section.

Now one must consider the **coherence** effect coming from summing over nucleons. Nuclear physicists knew all about coherence effects in atomic interactions... but they're all old and wrinkly now. In this day and age, we have to invoke highfalutin ideas like decoupling: as good effective field theorists, we know that the nuclear scale is 'macroscopic' relative to the dark matter scale. We thus have to ask if it it is appropriate to sum the quantum mechanically over the amplitudes coming from each target nucleon. This is a question of energy dependence since higher energies probe smaller scales. We already know from our discussion of the WIMP velocity distribution that

[9] This would be a novel topic for a future different A-exam, e.g. for Bibhushan Shakya.

WIMPs are very non-relativistic in the lab frame so that they have a large de Broglie wavelength that indeed probes the *entire* target nucleus.

We harp upon this because this already provides a dramatic simplification. It is not surprising that an electrically neutral dark matter particle should couple in (roughly) the same way to the proton and neutron since these are related by isospin. Thus we may take $f_p = f_n \equiv f$ and note that the first term in (3.9) takes the form

$$\hat{\sigma}_N|_{\rm SI} \approx \frac{4m_r^2}{\pi} f^2 A^2, \tag{3.10}$$

i.e. the spin-independent cross section is enhanced by a factor of A^2 due to coherence. Further, since spins form anti-parallel pairs in ground state nuclei, most of the spin-dependent cross section cancels and only leaves a leftover coupling to an odd number of protons or neutrons in the nucleus. Thus for our garden-variety WIMP interacting with a garden-variety (e.g. Ge) target with low spin, we can completely neglect the spin-dependence,

$$\hat{\sigma}_N \approx \hat{\sigma}_N|_{\rm SI}\,. \tag{3.11}$$

We remark that this simplification (assumed in standard direct detection exclusion plots) provides a place for the DAMA results to hide since DAMA's NaI target is much more sensitive to spin-dependent coupling than other direct detection experiments of comparable volume[10].

3.4 Differential recoil rate, a first pass

Let us now turn to the kinematics of the process. We assume elastic scattering since this dominates for point-like dark matter interacting with nuclei. This assumption provides another place to hide DAMA results, c.f. inelastic dark matter [88]. In the center of mass frame,

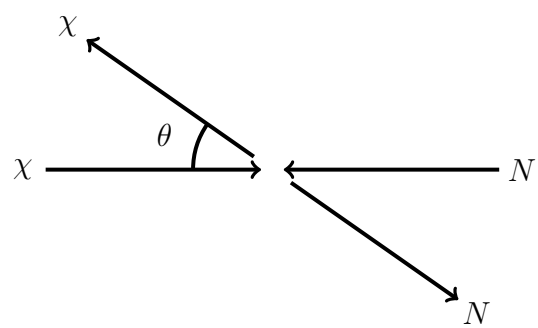

The kinematics of this scattering process are worked out thoroughly in first-year mechanics[11],

$$E_R = E_i r\,\frac{1-\cos\theta}{2}, \tag{3.12}$$

[10] I know this is being read by LHC physicists, so I should say that detector volume $\sim$ [instantaneous] luminosity.

[11] This would be an excellent Q-exam question, but since this committee has already given me a thorough Q-exam, think it is not necessary to ask me to derive this—right?

where r is a kinematic factor built out of the particle masses

$$r = \frac{4m_r}{m_\chi m_N} = \frac{4m_\chi m_N}{(m_\chi + m_N)^2}. \tag{3.13}$$

The key feature is that $0 < r \leq 1$ with the upper bound saturated for $m_\chi = m_N$. In other words, recoil energy is maximized when the masses of the WIMP and target nuclei are matched. The conventional cartoon to understand this is to consider the scattering of ping pong balls and bowling balls.

Now let us proceed to calculate the differential recoil rate for the case of zero momentum transfer $q = 0$ where we've already parameterized the relevant cross section. We will later correct for the q-dependence in the form factor. In the center of mass frame the scattering is isotropic so that E_R is uniform in $\cos\theta$ over the range

$$0 < E_R \leq E_i r = E_R^{\max}. \tag{3.14}$$

This gives us a relatively boring plot of differential recoil rate for an incident energy

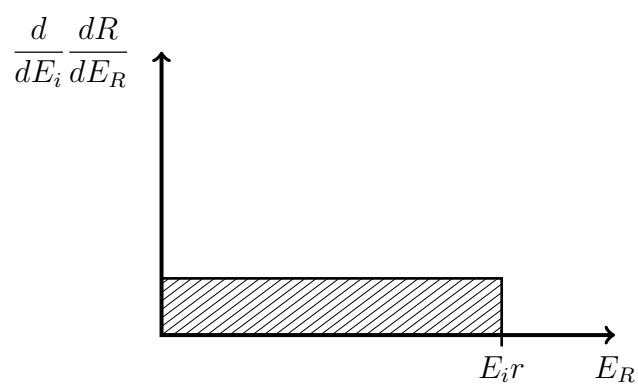

Nondescriptness notwithstanding, it is important to understand what is being plotted here. The vertical axis gives the rate of nuclear recoils for a sliver of recoil energies between E_R and $E_R + dE_R$ and a sliver of incident energies between E_i and $E_i + dE_i$. This is the differential of the recoil energy spectrum for the distribution of input WIMP velocities (i.e. E_i). The area of the shaded box represents the contribution to this differential rate coming from integrating over E_R for a given E_i. As promised this distribution is flat due to isotropy. The length of the box is given by $E_R^{\max}(E_i)$. The height of the box is a function of our zero momentum transfer cross section $\hat{\sigma}_N$ and E_i through the dependence of the rate on the WIMP velocity distribution. Thus we may write

$$\frac{d}{dE_i}\frac{dR}{dE_R} = \frac{\text{area}}{\text{length}} = \frac{dR}{E_i r}. \tag{3.15}$$

We would have a boring rectangular plot like this for *each* incident velocity (i.e. each E_i). The length of each rectangle is $E_i r$ and the height will be a more complicated function (given below) of the velocity distribution. In order to get the recoil spectrum, dR/dE_R, we can imagine stacking all of these boring rectangular plots on top of each other:

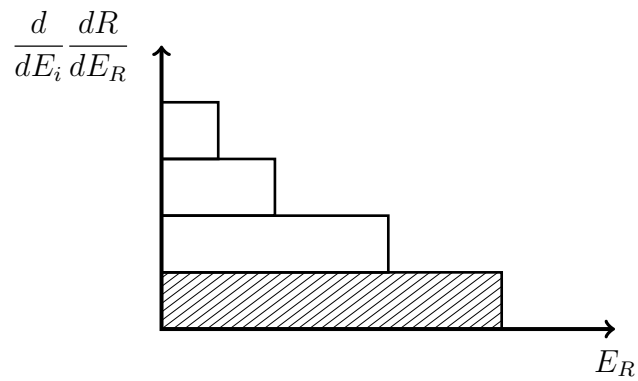

Now we can imagine summing together the contribution from each box to get the recoil spectrum, i.e. we can integrate (3.15)

$$\frac{dR}{dE_R} = \int_{E_i^{\min}}^{E_i^{\max}} \frac{dR(E_i)}{E_i r} \longrightarrow \int_{\vec{v}} \frac{dR(\vec{v}+\vec{v}_E)}{E_i r}, \tag{3.16}$$

where on the right we convert to an integral over WIMP velocity, i.e. $E_i = E_i(\vec{v}+\vec{v}_E)$. As we noted above when normalizing the Maxwellian velocity distribution, we have been glib about the limits of integration. To simplify our first pass, will take $E_i^{\max} \to \infty$ and $E_i^{\min} = E_R/r$ from the second inequality in (3.14). We will later address the effect of a finite $E_i^{\max}$ coming from the characteristic escape velocity $v_{\rm esc}$ of WIMPs in the dark matter halo.

To perform this integral we need an explicit form of the differential rate $dR(E_i)$ of scattering from an incident energy E_i to a recoil energy E_R. (We have only explicitly written the argument that is integrated over.) $dR(E_i)$ tells us how many such recoil events occur per kilogram-day of a target material of atomic mass A. Heuristically this is written as

$$dR = \frac{\#\text{ nuclei}}{\text{kg}} \cdot \frac{\text{rate}}{\text{nucleus}}, \tag{3.17}$$

i.e. the number of nuclei per unit mass multiplied by the rate per nuclei. To determine this latter quantity we can imagine each target nucleus traveling through space at velocity $\vec{v}_{\rm gal} = \vec{v}+\vec{v}_E$ in the WIMP rest frame with a cross section $\hat{\sigma}_N$.

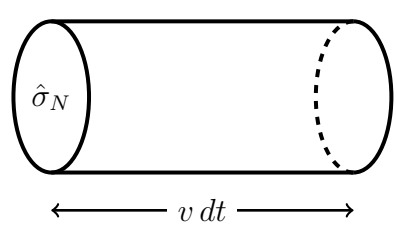

The nucleus effectively carves out an interaction volume $\hat{\sigma}_N v\,dt$ across a space with WIMP number density $n_0 f(\vec{v}+\vec{v}_E)\,d^3\vec{v}$. Thus the number of events is

$$\frac{\text{rate}}{\text{nucleus}} dt = \hat{\sigma}_N v_{\rm gal}\, n_0 f(\vec{v}+\vec{v}_E)\, d^3\vec{v}\, dt, \tag{3.18}$$

and the rate per nucleus is given by dropping the dt.

Plugging everything into (3.17), including the Maxwellian velocity distribution (3.2),

$$dR = \frac{N_0}{A} \cdot \hat{\sigma}_N v_{\rm gal}\, n_0 \frac{1}{k} e^{(\vec{v}+\vec{v}_E)^2/v_0^2}\, d^3\vec{v}, \tag{3.19}$$

where N_0 is Avogadro's number. Let us now perform the integral (3.16) in a very simplified 'toy' case which we will gradually make more sophisticated. In addition to setting $v_{\rm esc} \to \infty$, let us turn off the annual modulation from the Earth's motion in the galaxy, $\vec{v}_E = 0$ (this also sets $v_{\rm gal} = v$). The resulting integral is then

$$\frac{dR}{dE_R} = \int_{v_{\rm min}}^{\infty} \frac{1}{(\frac{1}{2}m_\chi v^2) r} \frac{R_0}{2\pi v_0^4} v\, e^{-v^2/v_0^2}\, 4\pi v^2\, dv. \tag{3.20}$$

The first term is just $(E_i r)^{-1}$, the second term defines R_0 to absorb constants in a way that will be convenient later, and the remainder contains the v dependence of dR. The minimum velocity is given by

$$E_i^{\rm min} = \frac{E_R}{r} = \frac{1}{2} m_\chi v_{\rm min}^2. \tag{3.21}$$

Proceeding to simplify and perform the integral,

$$\frac{dR}{dE_R} = \frac{R_0}{r\left(\frac{1}{2}m_\chi v_0^2\right)} \int_{v_{\rm min}}^{\infty} \frac{2}{v_0^2} e^{-v^2/v_0^2}\, v\, dv = \frac{R_0}{E_0 r} e^{-E_R/E_0 r}, \tag{3.22}$$

where we have defined $E_0 = \frac{1}{2}m_\chi v_0^2$ to be the most probable incident WIMP energy and R_0 can now be simply interpreted as the *total* rate for isotropic nuclear recoil from a non-relativistic point-like particle moving through the galaxy. Explicitly writing in all of the factors that went into this constant, we find

$$R_0 = \frac{2}{\sqrt{\pi}} \frac{N_0}{A} n_0 \hat{\sigma}_N\, v_0 \approx \frac{500\ \text{GeV}}{A\, m_\chi} \cdot \frac{\hat{\sigma}_N}{1\ \text{pb}} \cdot \frac{\rho_{\rm DM}}{0.4\ \text{GeV/cm}^3} \cdot \frac{\text{events}}{\text{kg day}}. \tag{3.23}$$

Sometimes people define silly units like tru ('**total rate unit**') = event kg^{-1} day^{-1} for this rate or the dru ('**differential rate unit**') for event kg^{-1} day^{-1} keV^{-1} [103]. However, the last thing particle physics needs is more units so we will not use these.

It is useful to pause for a moment to admire this toy result since it already gives a very rough estimate for what one might expect in the real world. Given a 100 kg detector made up of Xe ($A \approx 100$) and a 100 GeV WIMP with typical weak-scale nuclear cross section $\hat{\sigma}_N \sim 1$ pb, one ends up with about 5 events per day. This scales linearly with cross section, WIMP density (astrophysics), and inversely with the WIMP mass. Now suppose the target nucleus happens to have the same mass, $m_N = m_\chi = 100$ GeV (this is the right ballpark for Xe) so that $r = 1$, then we can calculate the mean recoil energy,

$$\langle E_R \rangle = E_0 r = \frac{1}{2} m_\chi v_0^2 = \frac{1}{2} 50\ \text{GeV}\ (.75 \cdot 10^{-3}) \approx 30\ \text{keV}. \tag{3.24}$$

This number is remarkably *small*, even though we're in the 'best case' scenario where the WIMP and target masses are matched. To compare to experiments that collider physicists (especially those at Fermilab) might appreciate a bit better, neutrino beam experiments typically detect events of MeV-scale energies. Dark matter experiments have to be significantly better than this.

3.5 Comparing apples to apples

Before moving on to make our toy model more realistic, let us pause to make an important point about meaningful ways to convey the information from a direct detection experiment. Assuming we have run such an experiment for some time and have detected no signal, we can make an exclusion plot to convey what our experiment has learned. We present such a plot in Fig. 2. The plot assumes that there are no events detected within the energy threshold; effectively one assumes that there was a maximal number of events of energy less than the threshold that would still be consistent with no observed events above threshold. Integrating (3.22) gives such a value for R for which one can plot $R_0/r \sim \hat{\sigma}_N$ over m_χ. One can qualitatively understand the features of this graph: at the minimum the kinetic factor r is maximized for $m_\chi \approx m_N$. Below this value there's not enough kinetic energy transferred (ping pong balls don't transfer much energy to bowling balls) and above this value the density of dark matter decreases ($n \sim \rho/m_\chi$) so that the bounds away from $m_\chi \approx m_N$ become weaker.

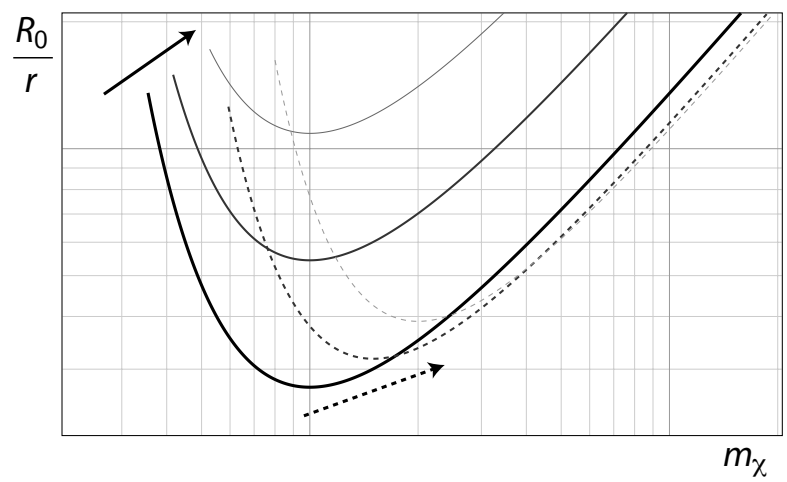

Figure 2: Model log-log exclusion plots from (3.22) in arbitrary units. Each line excludes points above it. Solid lines indicate increasing energy threshold (worse sensitivity) following the solid arrow while the dashed lines indicate increasing target atomic mass A. These plots were generated by the author, which should be taken as evidence that he knows what he's talking about.

Such a plot can be generated for each direct detection experiment with null results. The key question is how one ought to combine the results of different experiments. Since we know that different experiments use different target material (and this is good since this provides sensitivity for a broad range of WIMP masses), we are particularly concerned about the dependence of the exclusion plot on the target. This can be summarized by fact that we are setting bounds on the [zero momentum transfer] WIMP-*nucleus* cross section $\hat{\sigma}_N$ for various WIMP masses. This clearly is not a useful quantity when comparing experiments with different target nuclei. Fortunately, there is a trivial fix: rescale everything so that we provide bounds on the WIMP-nucle*on* cross section $\hat{\sigma}_n$ which is thus independent of the particular nucleus. Note that we use the convention that lowercase n refers to nucleon (or 'neutron') while capital N refers to the entire nucleus. The

conversion is straightforward,

$$\hat{\sigma}_N = \frac{m_r^2}{m_{rn}^2} A^2 \hat{\sigma}_n, \tag{3.25}$$

where m_{rn} is the reduced mass for the WIMP-nucleon system. Note that we pick up an additional factor of A^2 which, combined with (3.10), gives us a total coherence enhancement of A^4 in the WIMP-nucleon rate (the rate which is sensible to compare between experiments). Let us remind ourselves that we are restricting ourselves to the case of dominant spin-independent interactions, the case where spin-dependent scattering is appreciable requires more caution.

Plugging this back into our very rough (back of a very small envelope) estimate (3.23) and using $m_r^2/m_{rn}^2 \sim A^2$, we find that for our 100 kg Xe detector and 100 GeV WIMP, we get five events per day for a zero momentum transfer WIMP-nucle*on* cross section of $\hat{\sigma}_n \sim 10^{-8}$ pb.

3.6 More realistic velocities

The differential recoil rate in Section 3.4 is a handy estimate for what one would expect for an experiment, but it is a dramatic simplification. Let us make our toy expression slightly more sophisticated by taking into account the effect of a finite escape velocity and replace the effect of the Earth's annually modulated velocity relative to the dark matter halo. To make it clear which spectrum we are referring to, let us write

$$\frac{dR}{dE_R} \longrightarrow \frac{dR(v_E, v_{\rm esc})}{dE_R}, \tag{3.26}$$

where we explicitly write the dependence on the Earth's velocity and the escape velocity. The toy-model spectrum we derived above then $dR(0,\infty)/dE_R$.

Because the dark matter halo is gravitationally bound, there is a characteristic escape velocity at which the Maxwell distribution necessarily breaks down since any particles with such energies would escape the halo. Thus our integration over WIMP velocity (or, equivalently, incident energy) should have some upper limit. Technically, the gravitational potential modifies the Maxwell distribution at its tail, but it is typically sufficient to impose a hard cutoff. Typically $v_{\rm esc} \approx 600$ km s^{-1} should be used as the upper limit for the integration in (3.22). Note that this also requires a modification of the overall normalization of the Maxwell distribution. We define the finite $v_{\rm esc}$ normalization by

$$k_{\rm esc} = k_0 \left[{\rm erf}\left(\frac{v_{\rm esc}}{v_0}\right) - \frac{2}{\sqrt{\pi}} \frac{v_{\rm esc}}{v_0} e^{-v_{\rm esc}^2/v_0^2} \right], \tag{3.27}$$

where the error function is a convenient shorthand for the integral over the finite velocity domain. The modified recoil spectrum can be written in terms of the $v_{\rm esc} \to \infty$ spectrum as

$$\frac{dR(0, v_{\rm esc})}{dE_R} = \frac{k_0}{k_{\rm esc}} \left[\frac{dR(0,\infty)}{dE_R} - \frac{R_0}{E_0 r} e^{-v_{\rm esc}^2/v_0^2} \right], \tag{3.28}$$

where we see the effect of the rescaled normalization and an additional term which vanishes in the $v_{\rm esc} \to \infty$ limit. Let us remark that typically these large velocity effects are negligible relative

to our toy model since our garden-variety WIMPs tend to be rather heavy and don't carry much kinetic energy. This allowed us, for example, to simply truncate the distribution above the escape velocity. However, the light WIMP candidates introduced in Section 2.7 can populate more of the tail of the velocity distribution and proper treatment of this region is important [104].

Now let us account for the modulated velocity of the Earth relative to the dark matter halo, which we wrote above as:

$$v_E = 232 + 15 \cos\left(2\pi \frac{t - 152.5 \text{ days}}{365.25 \text{ days}}\right) \text{ km s}^{-1}. \tag{3.29}$$

Due to the unfortunate placement of our solar system in the Milky Way galaxy, the average velocity (232 km/s) is not very well known, though the amplitude of the modulation (15 km/s) is well measured. We should further remark that there are small errors since the modulation isn't exactly sinusoidal. This modulation clearly does not affect the finite v_{esc} term in (3.28) since the large v_{esc} dominates over v_E. However, this *does* affect the $dR(0,\infty)/dE_R$ term. Going through the same analysis as Section 3.4 with $v^2 \to (\vec{v} + \vec{v}_E)^2$, we find

$$\frac{dR(v_E,\infty)}{dE_R} = \frac{R_0}{E_0 r}\frac{\sqrt{\pi}}{4}\frac{v_0}{v_E}\left[\text{erf}\left(\frac{v_{\text{min}} + v_E}{v_0}\right) - \text{erf}\left(\frac{v_{\text{min}} - v_E}{v_0}\right)\right]. \tag{3.30}$$

Combining this with (3.28) finally gives us

$$\frac{dR(v_E, v_{\text{esc}})}{dE_R} = \frac{k_0}{k_{\text{esc}}}\left[\frac{dR(v_E,\infty)}{dE_R} - \frac{R_0}{E_0 r}e^{-v_{\text{esc}}^2/v_0^2}\right]. \tag{3.31}$$

This certainly brings us closer to a realistic expression (though we still have not included q-dependence), but (3.30) and (3.31) leaves much to be desired in terms of having something tractable to interpret. Fortunately, it turns out that (3.30) can be approximated very well by a simpler form,

$$\frac{dR(v_E,\infty)}{dE_R} = c_1 \frac{R_0}{E_0 r} e^{-c_2 E_R/E_0 r}, \tag{3.32}$$

for some fitting 'constants' c_1 and c_2 which vary slightly with the time of year

$$.73 \le c_1 \le .77 \qquad\qquad .53 \le c_2 \le .59. \tag{3.33}$$

A detailed time-dependence can be found in Appendix C of [103], but for most cases it is sufficient to set them to their average values $\langle c_1 \rangle = 0.75$ and $\langle c_2 \rangle = 0.56$. Note that these are not independent, since integration of the above equation forces $c_1/c_2 = R(v_E,\infty)/R_0$. In this simplified form we can see that the that the effects of the Earth's motion can increase rate and make the spectrum slightly harder (from c_2).

Finally, let's remark that integrating the spectrum (3.30) to get a total rate and differentiating with respect to the Earth's velocity gives

$$\frac{d}{dv_E}\left(\frac{R}{R_0}\right) = \frac{1}{v_E}\left[\frac{R}{R_0} - \frac{\sqrt{\pi}v_0}{2v_E}\text{erf}\left(\frac{v_E}{v_0}\right)\right] \approx \frac{1}{2v_E}\frac{R}{R_0}, \tag{3.34}$$

where our final approximation assumes $v_E \approx v_0$. From this we can see that the 6% modulation in v_E causes a 3% modulation in the rate. A nice plot of this effect is show in Fig. 3.

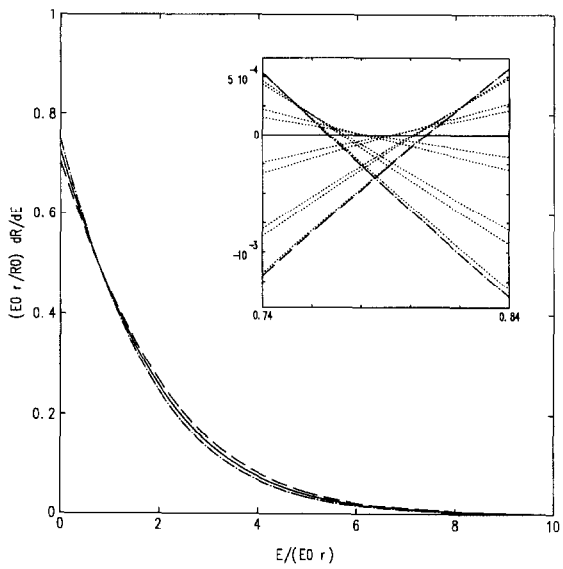

Figure 3: Plot of $dR(E_R)/dE$ showing the seasonal variation of the rate spectrum. The solid line is the annual average, dashed line is June, dotted-dashed line is December. The inset shows an enlargement of the crossover region with the annual average subtracted. Dotted lines in the inset are monthly averages. Image from [103].

3.7 Form factor suppression: coherence lost

Perhaps the most obvious omission in our toy model thus far has been the approximation of zero momentum transfer, $q = 0$. This came from our ansatz all the way back in (3.7) that we could reliably treat the q-dependence as a correction to the $q = 0$ cross section which we parameterized as a form factor, $F(q)$. Now we should justify this parameterization and determine the form of $F(q)$. See [107] for a discussion.

Momentum transfer from the WIMP-nucleus collision is

$$q = \sqrt{2m_N E_R}. \tag{3.35}$$

For large enough values of q we expect coherence to break down as the de Broglie wavelength becomes smaller than the scale of the nucleus. A simple way to develop an intuition for the form factor is to work in the first Born approximation (i.e. plane wave approximation):

$$\mathcal{M}(q) = f_n A \int d^3\vec{x}\, \rho(\vec{x}) e^{i\vec{q}\cdot\vec{x}}, \tag{3.36}$$

where ρ is the density distribution of scattering sites. The form factor is precisely the this Fourier transform over the scattering lattice,

$$F(q) = \int d^3\vec{x}\, \rho(x) e^{i\vec{q}\cdot\vec{x}} = \frac{4\pi}{q} \int_0^\infty r\, \sin(qr)\, \rho(r)\, dr. \tag{3.37}$$

For spin independent interactions, a simple model of the nucleus as a solid sphere turns out to be

a very good approximation. In this case the form factor takes the form

$$F(qr_N) = \frac{j_1(qr_N)}{qr_N} = 3\frac{\sin(qr_N) - qr_N\cos(qr_N)}{(qr_N)^3}, \tag{3.38}$$

where we've written the momentum dependence in terms of a dimensionless quantity qr_N where $r_N \sim A^{1/3}$ is a characteristic nuclear radius. Recall that $q \sim \sqrt{AE_R}$ where the A-dependence comes from $m_N \sim A$. Thus the leading A and E_R dependence of qr_N goes like

$$qr_N \sim A^{5/2}E_R^{1/2}. \tag{3.39}$$

A more accurate parameterization from [103] is

$$qr_N = 6.92 \cdot 10^{-3}A^{1/2}\left(\frac{E_R}{\text{keV}}\right)^{1/2}\left(a_N A^{1/3} + b_N\right), \tag{3.40}$$

where a_N and b_N are 'fudge factors' to give the correct nuclear radius r_N from its A dependence. We will simply take $a_N = 1$ and $b_N = 0$ (to this precision $6.92 \to 7$) so that a reasonable-to-detect 100 keV recoil of a Xe ($A \approx 100$) nucleus gives $qr_N \approx 3.2$. From our argument about length scales one might worry that this is the regime where coherence breaks down. Indeed, plugging into our solid sphere nuclear model, we get an $F^2(qr_N)$ suppression as plotted in Fig. 4.

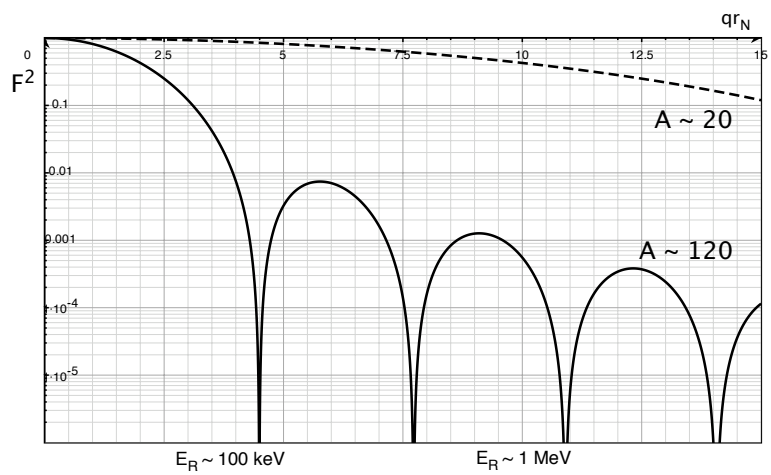

Figure 4: Form factor suppression $F^2(qr_N)$ on a log plot. Solid line: F^2 suppression for fixed $A \sim$ 120 over different recoil energies and corresponding qr_N values on the top axis. Dashed line: F^2 suppression for fixed $A \sim 20$ for the same recoil energies. (Note: the qr_N values for the dashed lines are related to the top axis by an additional factor of ~ 0.2.)

We see that for light target nuclei, the form factor doesn't make much difference. For heavy nuclei, on the other hand, we can resolve the structure of the Bessel function (the Fourier transform of our solid sphere nuclear model) and we find ourselves hitting the zeroes of j_1 and brushing up against its exponential suppression.

This is a very important plot to take into account when designing a direct detection experiment. We saw in (3.10) that the spin-independent nuclear cross section scales as A^2. This is enhanced

to A^4 when considering the more useful nucleon cross section. While we know that having too large an A (so that $m_N \gg m_\chi$) leads to penalty in the kinetic factor r, we know from (3.13) that this is only A^{-1}. Thus it would still seem advantageous to build detectors with the heaviest target materials available to maximize the interaction cross section. As we've now seen (and could have expected), this breaks down when the WIMP is no longer able to scatter coherently off the entire nucleus. One must then balance the coherence from having heavy nuclei with the form factor suppressing coming from decoherence.

As we consider larger nuclei (large A), the region around $q = 0$ where $F^2(qr_N)$ is not prohibitive becomes smaller. The trade off when designing an experiment then depends crucially on how low one can push the energy threshold: what is the smallest nuclear recoil that one can measure? If you can efficiently detect arbitrarily low threshold recoils, then you can go ahead and use the heaviest nuclei you can find for your detector. However, real experiments only have a finite energy threshold (partially a function of the target material). For this minimum recoil energy, one must consider to what extent the form factor suppression from one's target material will suppress one's signal.

Thus in Fig. 4, the $A \sim 20$ detector takes a big hit in the interaction cross section because of its low A value. However, we see that one is free to use a detector technology with a less prohibitive energy threshold since F^2 doesn't decrease very quickly. The $A \sim 120$ detector, on the other hand, gives a nice enhancement from coherence, but *only* for sufficiently low energy recoils so that one must be very sensitive to low energy signals. As a rule of thumb, targets lighter than Ge start start to lose a lot from A^2 suppression; i.e. current detector technology does not require A any lower than this to ensure reasonable efficiency.

This is an important lesson to put the CDMS and XENON experiments in context. While Xe is appreciably heavier than Ge, form factor suppression (decoherence) in Xe leads to the two being roughly the same in their ability to detect WIMPs.

Failure for spin-dependent case: see [11] of LS [107, 108]

3.8 Further refinement

If you are doing everything well, you are not doing enough.
– Howard Georgi, personal motto [109]

In addition to proper inclusion of spin-dependence and refinements of the models used above (e.g. the halo, Born approximation with a hard sphere), a good and honest experimentalist ought to properly consider the effects of detector resolution and statistics. (Un-)Fortunately, as a theory grad student I am neither particularly good nor honest when it comes to such matters and I will leave their detailed discussion to pedagogical expositions in [103] and [70]. Let us briefly address some salient effects.

Detection efficiency. First on the list of experimental considerations is the efficiency at which the nuclear recoil energy is detected. As we already know, nuclear recoils and electron recoils are very different interactions. Given an electron and a nuclear interaction with the *same* recoil energy, a given detector technology will measure different values for such events due to the nature of the detection technique (we will mention canonical examples below). This means that instead of the spectrum with respect to the recoil energy dR/dE_R, one should calculate the

spectrum with respect to the *visible* energy dR/dE_v where $E_v = f_n E_R$ so that

$$\frac{dR}{dE_R} \approx f_n \left(1 + \frac{E_R}{f_n}\frac{df_n}{dE_R}\right)\frac{dR}{dE_v}. \tag{3.41}$$

A related issue that is important to discuss is **quenching**[12]; see [8] for a nice discussion. Because detectors respond differently to nuclear recoils than to electron recoils, we need useful units to measure our visible energy. The difference between the visible energy coming from electron and nuclear events of the same recoil energy is parameterized by a **quenching factor**, Q. This leads to some silly notation: $\mathrm{keV_{ee}}$ for the "electron equivalent" energy (i.e. observed energy had the event come from an electron) and $\mathrm{keV_r}$ for the energy signature from a "nuclear recoil."

$$E_e(\mathrm{keV_{ee}}) = Q \times E_r(\mathrm{keV_r}) \tag{3.42}$$

Energy resolution. The next effect to consider is the finite resolution for any real detector. This means that if there were *exactly* N signal recoils each of a single energy $E_v = E_v'$, then our real detector would observe a spread of energies smeared out in an approximately Gaussian manner with some energy-dependent width ΔE,

$$\frac{dN}{dE_v} = \frac{N}{\sqrt{2\pi}\Delta E} e^{(E_v - E_v')^2} 2\Delta E^2. \tag{3.43}$$

Thus the actual spectrum that we measure should be transformed to

$$\frac{dR}{dE_v} = \frac{1}{\sqrt{2\pi}} \int dE_v' \, \frac{1}{\Delta E}\frac{dR}{dE_v'} e^{(E_v - E_v)^2/2\Delta E^2}, \tag{3.44}$$

where $\Delta E(E_v') \sim \sqrt{E_v'}$. Real experimentalists should also 'fold in' the other terms in ΔE relevant to a given detector technology. For low energy events one should also worry that the Gaussian statistics above might lead to erroneous loss of counts due to negative energies. This can be solved by using a Poisson distribution, but leads to issues regarding the energy threshold.

Energy threshold. As discussed above, the most favorable rates come from low energy events where the de Broglie wavelength of the WIMP is large enough to permit coherent scattering against an entire target nucleus. However, detectors (e.g. photomultiplier tubes) can only resolve events above a given threshold energy. Noise reduction also sets a threshold dependent on nearby radioactive sources (e.g. impurities in the target material) and shielding. These cutoffs must be taken into account for each experiment when constructing exclusion plots.

Target mass fractions. Let us comment in passing that in detectors with compound targets (e.g. NaI for DAMA) one must calculate the rate limit separately for each target.

To summarize, let use write out the recoil spectrum with respect to *measured* energy as a handy mnemonic:

$$\frac{dR}{dE_v} = R_0 \sum_A f_A S_A F_A^2 I_A, \tag{3.45}$$

[12] Is it just me, or do experimentalists use this word to refer to *way* too many different phenomena?

where R_0 is the total rate, A runs over the relevant atomic mass numbers, f_A gives the detection efficiency for nuclear recoil, S_A is the spectral function, F^2 is the form factor suppression, and I_A is a reminder about which sort of interaction (spin-independent or spin-dependent) we are considering. S_A is essentially the spectrum in (3.22) modified by all of the above velocity and detector effects. It gives the same qualitative behavior as in Fig. 2.

4 Direct Detection: Experiments

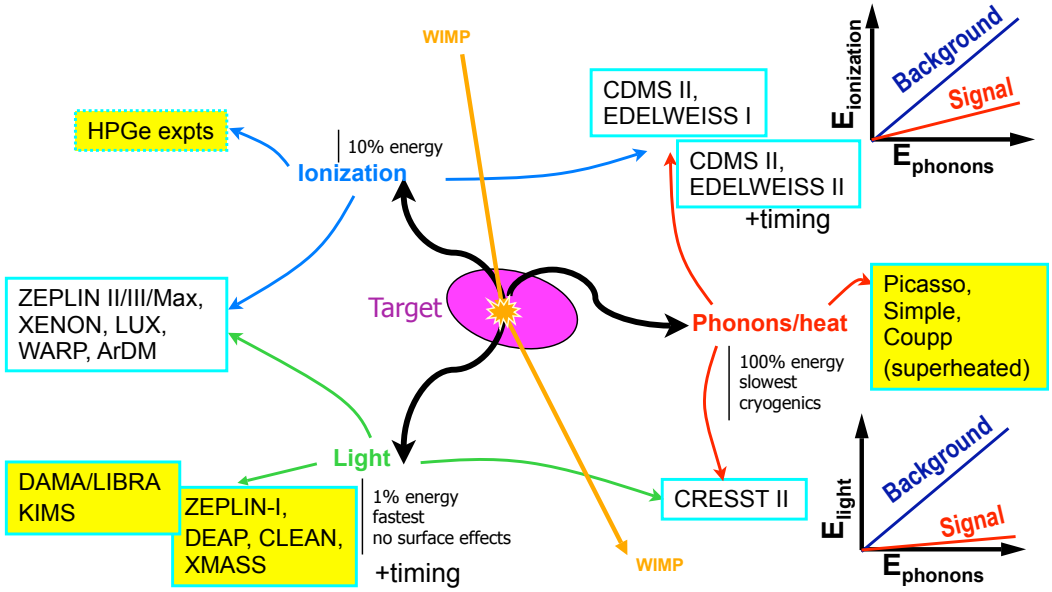

Figure 5: Image from Dan Akerib's lecture in [4], though this is used in several talks from CDMS collaboration and the original source is unclear.

Instead of cataloguing a long list of direct detection experiments, we will only highlight the distinguishing features between the primary experimental classes illustrated in Fig. 5. In this we will focus on the **cryogenic detectors** ('bolometers') operated at $T < 77$ K. These include solid state and superfluid ^{3}He detectors. In the following section we will go into further detail on the use of scintillation and ionization in liquid noble gas detectors such as XENON.

Cryogenic detectors marked the beginning of the modern search for dark matter via direct detection. At low temperatures these detector materials have a heat capacity which approximately follows a T^3 dependence following Debye law amking it possible to make real measurements of very low energy deposition (typical thresholds can be as low as 1 keV). These 'bolometer' detectors use a precise measurement of the temperature increase from a potential WIMP event to discriminate against background events. There is a typical 100 ms thermalization time which restricts bolometry sensitivity to low interaction rates, but this is precisely the scenario for WIMPs.

The main problem faced by direct detection experiments is background reduction. WIMP events are extremely rare and the nature of the signals can be ambiguous. Did a nuclear recoil

occur from a WIMP or a background neutron from a cosmic ray? Maybe it wasn't a nuclear recoil at all, but a gamma ray scattering off an electron? Background sources are portrayed in Fig. 6.

4.1 Backgrounds

Let's briefly mention some of the key kinds of background [110]. For a comprehensive review, see e.g. [111].

- γ **Radioactivity**. Gamma rays from the surrounding area and the detector apparatus itself. Particularly relevant examples are radioactivity in photomultipliers in scintillating detectors and the long-lived isotopes in the detector material from cosmic activation. Notable target materials that must deal with such isotopes include ^{39}Ar, ^{68}Ge (and ^{65}Zn in Ge). One can mitigate these effects with lead shielding separating the detection volume from the rest of the apparatus and by only considering a 'fiducial' target volume for a 'self-shielding' target that attenuates gamma rays. (We will discuss this further below.)

- β **Radioactivity**. β radiation from ^{210}Pb (a daughter of naturally occurring radon in the air) can lead to surface interactions which are best eliminated by 'fiducializing' detector volume. This is the reason why physicists working directly with dark matter detectors have to wear ridiculous-looking clean room "bunny suits."

- **Fast neutrons**. While photons and electrons interact primarily via electron recoil in the detector volume, neutrons from cosmic ray muons interacting with the Earth around a detector interact via nuclear recoil and can mimic the signal of a WIMP. An MeV scale neutron can give a $\sim$ 10 keV$_{\rm r}$ nuclear recoil signal after elastic diffusion. The primary difference between neutron and WIMP interactions are their cross sections so that one can somewhat discriminate against neutron signals by discarding multiple-recoil events. Polyethylene shielding can also be used to slow neutrons before they enter the detector volume. This source of background is the primary reason why WIMP experiments must be located deep underground.

- **Solar neutrinos**. The coherent diffusion of solar neutrinos through the target volume could also mimic a single-recoil WIMP singal. However, this is only expected to become relevant for very large volumes (e.g. the next generation detectors at the ton scale) and long exposure times. This should not be confused with solar neutrino searches for dark matter.

The main point is that the background rate completely dwarfs the WIMP interaction rate and forces experiments to go deep underground and employ techniques to discriminate background. As depicted in Fig. 5, modern detector make use of multiple detection mechanisms to provide a way to identify and reject backgrounds. This provides a way to classify detectors by their choice of detection technologies.

4.2 Heat and charge

The current spin-independent benchmark for direct detection comes from the CDMS II [68] experiment. These are able to detect *non*-thermal phonons on short time scales ($\sim$100 μs). To measure

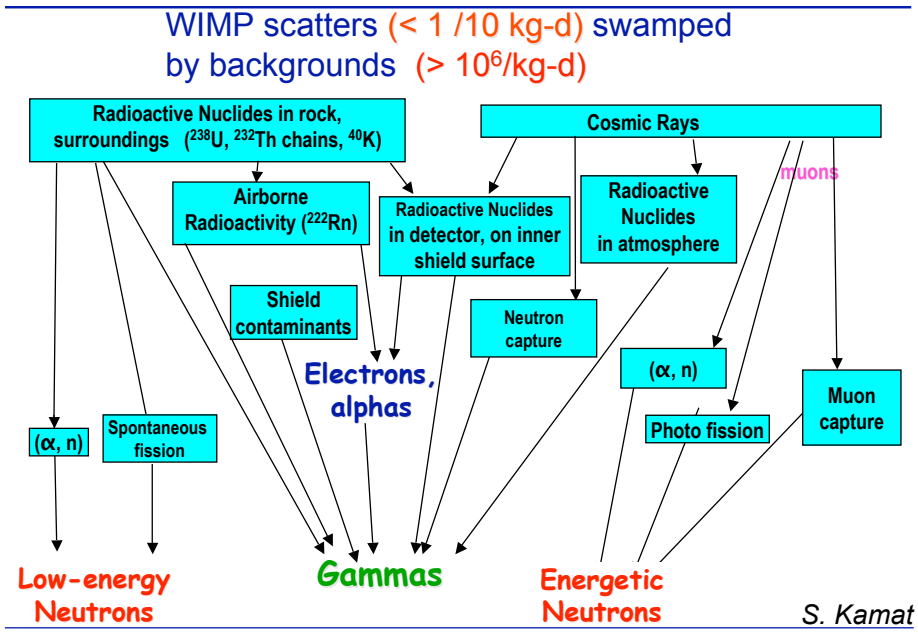

Figure 6: Examples of the primary sources of background for direct detection experiments. Image from [6], though this is used in several talks from CDMS collaboration and the original source is unclear. (Apparently it is from S. Kamat.)

the the ionizing effect of a nuclear recoil the target volume in placed an electric field with electrodes on the crystal surface. As a recoiling nucleus travels through the target volume it ionizes atoms. In semiconducting crystals this leads to electron-hole pairs, while in liquid and gaseous detectors this gives free electrons and ions. The electric field pulls the charges to the top and bottom of the surface where they can be detected by electrodes. The ionization yield of a gamma ray and the quenching factor for nuclear ionization is well understood so that a precise measurement of the ionization signal relative to the thermal signal can effectively reject electron-induced events. Particularly troublesome events are those where charge is not accurately collected, e.g. interactions close to the electrode surface. This can lead to electron recoil events which appear to be nuclear recoils.

CDMS rejects these events by simultaneously measuring phonon signals in the target crystal as an orthogonal discriminator against background events. A combination of signal timing, heat pulse shape, and relative pulse and ionization are used in addition to the ionization energy to reduce backgrounds.

4.3 Heat and light

Instead of ionization, an alternative detection mechanism is to use a scintillating material which emits photons as a recoiling nucleus passes through it. This photon signal is detected by a photomultiplier tube and can be used to discriminate between nuclear and electronic recoils. Scintillation materials can be purified to achieve low radiation contamination, though special care is necessary to reduce background from the photomultiplier glass itself (due to uranium and thorium content). The most popular options for scintillating materials are NaI(Tl) and Xe, which

one should immediately associate with the DAMA and XENON experiments. These have the benefit of having large A and being easily purified. Experiments must also couple scintillation method with an alternative form of detection (e.g. phonons) to reduce background.

4.4 Light and charge

The remaining combination of detection mechanisms are light (photons) and charge (ionization). The natural candidates for this sort of detector are the noble liquids, xenon and argon. The principles of so-called time projection chambers using xenon is the subject of the next section.

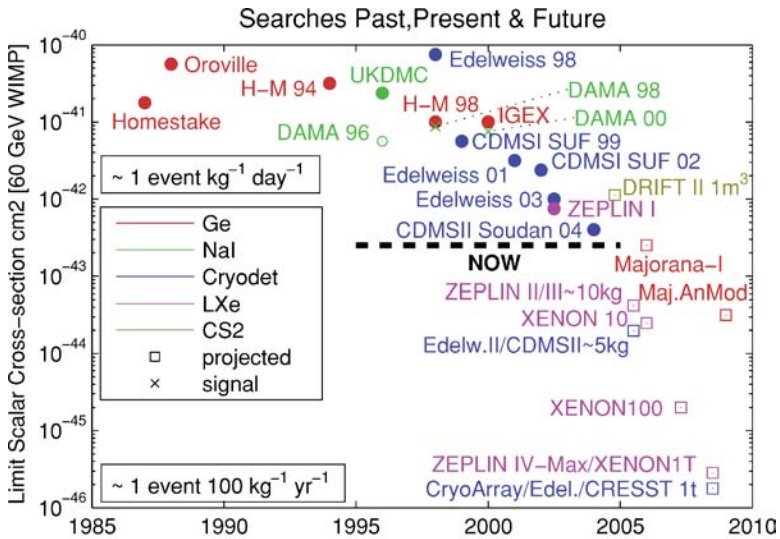

Figure 7: A plot of "past, present, and future" direct detection experiments with limits from 2004 [8]. Plotted are the 90% upper confidence level limits for different experiments normalized to a 60 GeV WIMP in 'Ge-equivalent' rates with a threshold > 10 keV. Horizontal axis gives publication time. Note the time dilation effect that causes a projection in 2004 to anticipate future experimental results far earlier than they will actually be ready, c.f. the LHC.

5 The XENON experiment

Let us now present the XENON experiments. The XENON10 experiment ran form 2005-2007 and set a bound of $\sigma_{\rm SI} \leq 8.8 \times 10^{-44}$ cm^{-2} [112, 113]. The primary purpose of this A exam is to be prepared for the results of the XENON100 experiment to be announced this summer, it is expected to set bounds on the order of $\sigma_{\rm SI} \leq 2 \times 10^{-45}$ cm^{-2}. Finally, plans are underway to scale the experiment up to XENON1T with a fiducial volume on the order of a metric ton from 2011-2015 with the goal of setting a bound of $\sigma_{\rm SI} \leq 10^{-46}$ cm^{-2}. XENON is the current flagship effort for liquid noble gas detectors which utilize ionization and scintillation techniques to remove background events[13]. In case there's any confusion, XENON (in all capital letters) refers to the

[13]We will not discuss LUX, a similar experiment in the US. Most of the discussion about XENON translates to LUX.

experiment while xenon (lowercase) or Xe refer to the element. I don't know why the experiment capitalizes its letters—it does not appear to be an acronym for anything. We will also write LXe to refer to liquid xenon because this what all of the cool physicists do.

5.1 Xenon: what's inside XENON

Before discussing two-phase time projection chambers, let us remark on the properties of xenon as a dark matter detector. The first property that makes xenon an excellent detector material is it large atomic weight $A \approx 131$. As we learned from Section 3, this means that the spin-independent scattering cross section is enhanced ($\sigma_{\rm SI} \sim A^2$) *provided* that has a detector technology that is sufficiently sensitive to recoil energies, as we will see is the case for XENON. A plot of the event rate by recoil energy is given in Fig. 8 to give a sense of the sensitivity required to do better than germanium detectors like CDMS. Further, over 45% of naturally occurring xenon atoms are odd-spin isotopes (^{131}Xe and ^{129}Xe) which make them sensitive to spin-dependent coupling. In addition to being a 'big target,' xenon also has favorable features for background control. It has no long-lived radioactive isotopes so there is no bulk contamination except from ^{85}Kr, which can be reduced to the part-per-thousand level using commercial methods. Further, thanks to its high atomic number and density, xenon has excellent stopping power so that it is **self-shielding** against penetrating radiation. (As the XENON spokesperson puts it, "it's damn good.") We will see that the XENON collaboration makes use of this property by 'fiducializing' the detection volume to reduce background from events near the detector surface. Xenon remains liquid up to 165K so that it does not require extensive cryogenic systems. Combined with its relatively modest cost, this allows xenon-based detectors to be efficiently scaled to large volumes.

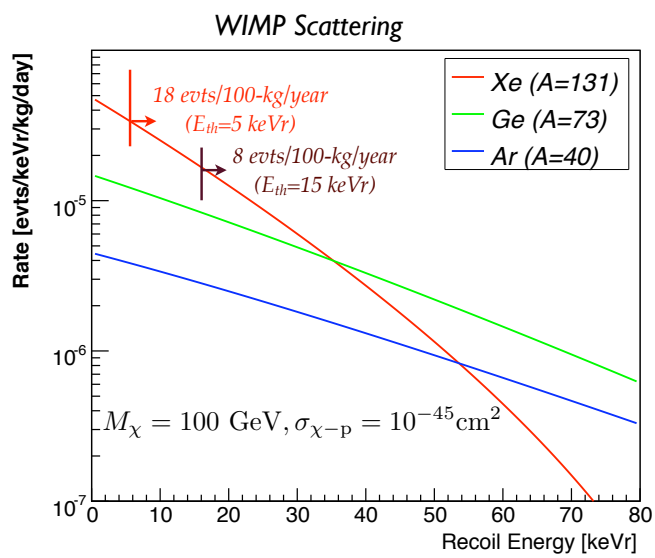

Figure 8: Spin-independnet Xe recoil rate plotted against Ge and Ar to provide a sense for how sensitive a Xe detector must be to low-energy recoils to avoid form factor suppression relative to other materials. Image from [114].

5.2 Light and Charge: Ionization and Scintillation

The energy of an incident particle in noble liquids goes primarily into ionization (and excitation of electrons liberated in ionization processes). Xenon is notable for having the lowest W-value of the noble gases, where

$$W = \frac{\langle \text{energy to produce an electron-ion pair} \rangle}{\text{ionization potential}}. \tag{5.1}$$

This means that xenon has the highest ionization yield of all the noble liquids, i.e. the largest signal. (This is especially important for spin independent measurements which are most sensitive to low recoil energies.) Representative ionization yields are shown in Fig. 9 for reference.

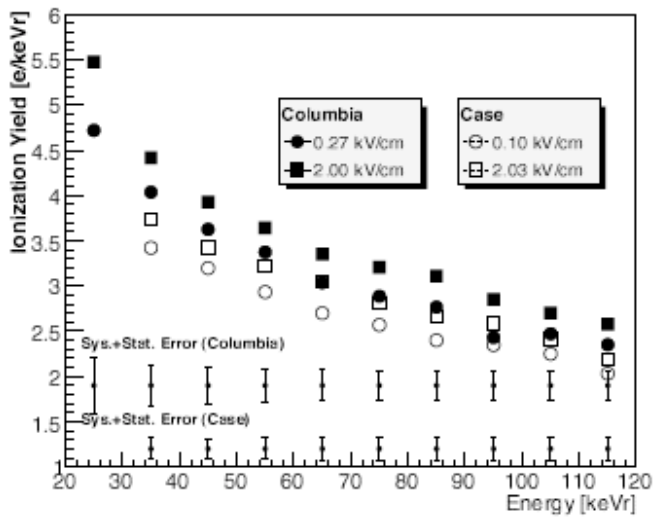

Figure 9: Ionization yield from nuclear recoils measured with small two-phase xenon detectors (labeled Columbia and Case). Xenon is sensitive to nuclear recoils of even a few keVr. The increase at low energies is believed to come from a drop in the electronic stopping power at low energies. Image from [115].

These ions are then detected via the **scintillation** light the ions return to their ground states. Scintillation occurs in noble liquids arises through the two channels (excitation and ionization) in Fig. 10. In both processes the excited dimer Xe_2^* (where Xe can be replaced with any other noble liquid) is de-excited to the dissociative ground state through the emission of a single [vacuum] ultraviolet photon. The scintillation light has two components coming from the de-excitation of the singlet and triplet dimer states. Fig. 11 shows the decay shape of scintillation signals in liquid Xe from various sources. The α and fission fragment sources the combination of the two decay shapes coming from the triplet and singlet states, while electrons only have one decay component as expected. While such 'pulse shape discrimination' can be used effectively in other liquid noble detectors (most notably argon), this is difficult in in liquid Xe due to the small time difference of the two decays.

Let us remark on a *different* source of scintillation light that will be particularly relevant for XENON and its class of "two phase time projection chamber" (TPC) detectors discussed below.

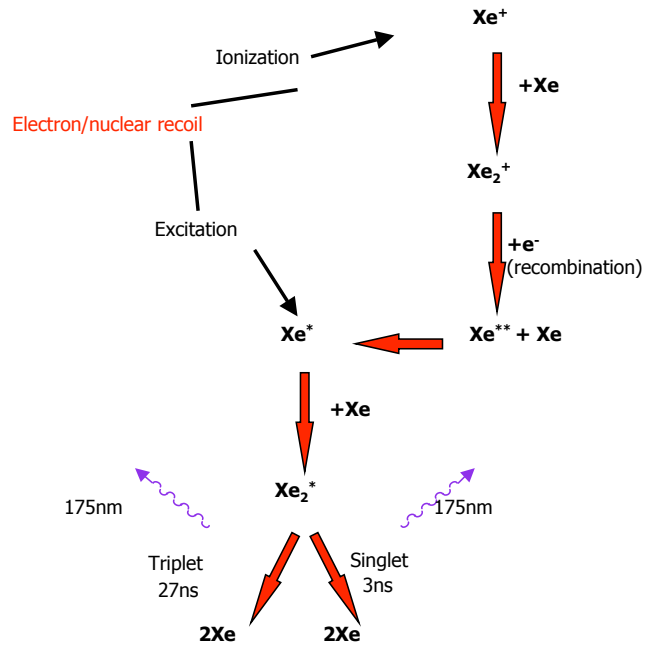

Figure 10: Sources of primary scintillation from ions and excited states of noble gases. Image from [6].

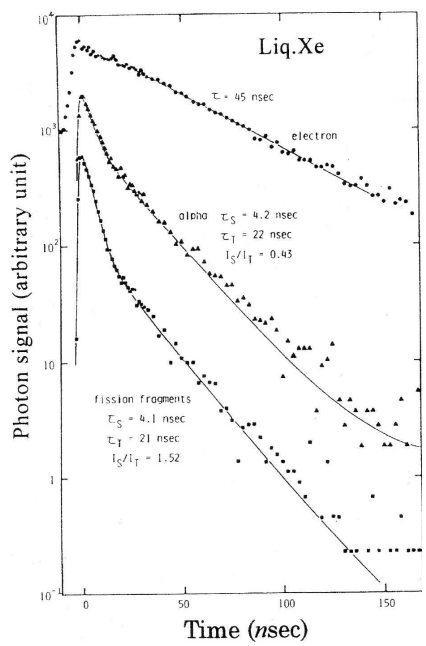

Figure 11: Decay curves of scintillation from liquid xenon excited by electrons, α particles, and fission fragments. Image from [115].

In a volume with both liquid and gas components, electrons liberated in LXe can be extracted via an electric field into the gas region. In the TPC detectors that we will be considering there is an additional field applied at the liquid-gas interface that causes **proportional scintillation** (or **electroluminescence**). We shall distinguish this from the **primary scintillation** in Fig. 11.

5.3 Two-Phase Time Projection Chamber

We note that while we advertised our detector as a 'light and charge' detector, one could now deduce from the above discussion that XENON is really a 'light' detector that is sensitive to both primary scintillation (what we called 'light' above) and proportional scintillation ('light' from charge). It is the relation between the initial primary signal—which is called S1—and the secondary proportional signal—called S2—that gives us the two independent measurements of each event that modern direct detection experiments rely on to discriminate electron from nuclear recoils. This is the basis of the so called **two-phase time projection chamber** (TPC) detectors.

We note that the S2 signal is always larger than the S1 signal due to the amplification at the liquid-gas interface. The ratio of S2 to S1, however, is larger for electron recoil and gamma ray interactions since these are more ionizing that nuclear recoil events. A cartoon of the XENON detector is shown in Fig. 12. The detector is composed of an upper and lower photomultiplier

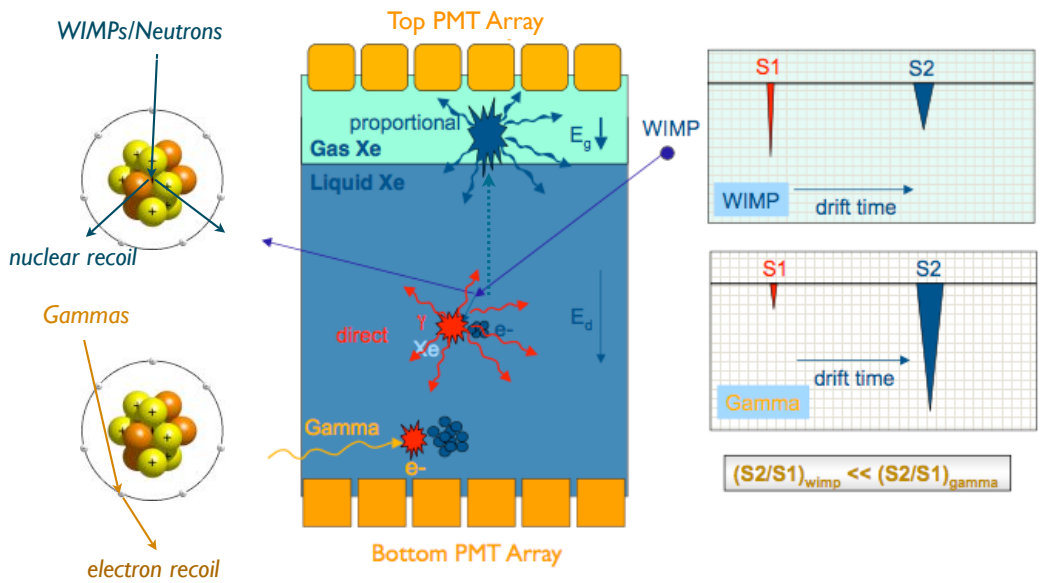

Figure 12: Image from Elena Aprile's presentations on behalf of the XENON collaboration [114], though this is used in several talks from XENON collaboration and the original source is unclear.

tube (PMT) arrays to detect scintillation light. The sides of the cylindrical volume are effectively mirrored to reflect scintillation light. Due to the different index of refraction in liquid and gaseous xenon, direct light in the liquid volume undergoes total internal reflection and so is detected primarily in the lower PMT array (immersed in the liquid). On the other hand, the upper photomultipliers detect proportional scintillation and provide $x - y$ event data. The drift time between the S1 and S2 events allows one to also determine the z-position of the event so that this

class of detectors provide full 3D event reconstruction. For more details on the applications of liquid xenon to particle and astroparticle physics, see [115]. To summarize:

- Primary scintillation occurs in the liquid and is detected by the lower PMT.
- Electrons liberated in ionizing processes are pushed across the liquid-gas boundary and are detected on the upper PMT array. This also determines the transverse location of the event.
- The relative size S1 and S2 signals provides a handle to discriminate electron/gamma events from dark matter candidates (nuclear recoils).
- The drift time between the S1 and S2 signals determines the longitudinal (z) position of the event.

5.4 Calibration and background

Let's now address the most important aspect of any dark matter search: getting rid of background. We've already discussed the basic features of the detector that help minimize background: shielding, light-and-charge detection, and a detection material that is 'intrinsically pure' with no long-lived radioactive isotopes (and commercial mechanisms to maintain the necessary purity).

The first source of additional background reduction comes from **fiducializing** the detector volume. I have no idea *why* they call it 'fiducializing,' but the idea is to make use of the time projection chamber's event-by-event 3D position determination to cut events that occur near the detector surface since this is where background photons are most likely to interact. (This, in part, is because of xenon's remarkable stopping power.) The background rate in the central part of the detector is five times smaller than that at the edges (0.6 events/KeVee/kg/day). This is shown in Fig. 13. After the fiducial volume cut nearly all background from PMTs and the detector wall (e.g ^{60}Co) are removed. One of the features of TPCs is that this efficiency improves with larger detector volumes.

Next we impose **energy selection** cuts. In Fig. 14 we present calibration data from XENON10 from Ce-137 (an electron source) and AmBe (a neutron source). The neutrons are meant to mimic dark matter recoils. As we have explained, the $S2/S1$ ratio (proportional scintillation over primary scintillation) differs for electron versus neutron recoils. In the figure we we see this difference explicitly. The discrimination strategy is to reject events that are above the nuclear recoil mean line. This rejects 99.5% of electron recoil events.

The energy cuts are based on calibration of the $S2/S1$ ratios. Compared to the calibration data in Fig. 14, one can subtract the energy-dependent mean $\log(S_2/S_1)$ of the electron-recoil band to obtain a $\Delta\log(S_2/S1)$ for each event. This flattens the band to Fig. 16. The energy window is divided into seven bins with an acceptance window defined by a Gaussian about the calibration mean for each bin. During calibration the collaboration found 'anomalous leakage' events coming from multiple-scatter events with one scatter coming from the nonactive LXe volume below the cathode (i.e. with no proportional scintillation). In such an event the $S2$ signal only comes from the scattering in the active volume while the $S1$ signal comes from both scattering events. This makes the $S2/S1$ ratio smaller and can push some events into the WIMP-search window. In order to remove such events additional cuts are imposed based on the $S1$ signal asymmetry between the top and bottom PMTs and the transverse-plane hit pattern of the $S1$ photons.

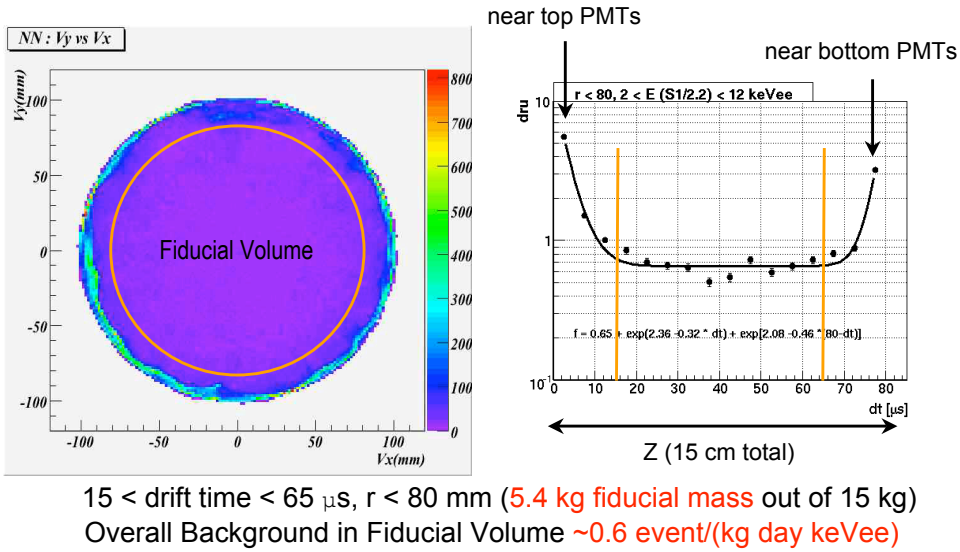

Figure 13: By exploiting 3D event information XENON can impose cuts on events that occur outside a 'fiducial volume' where background events are concentrated. Image from [114].

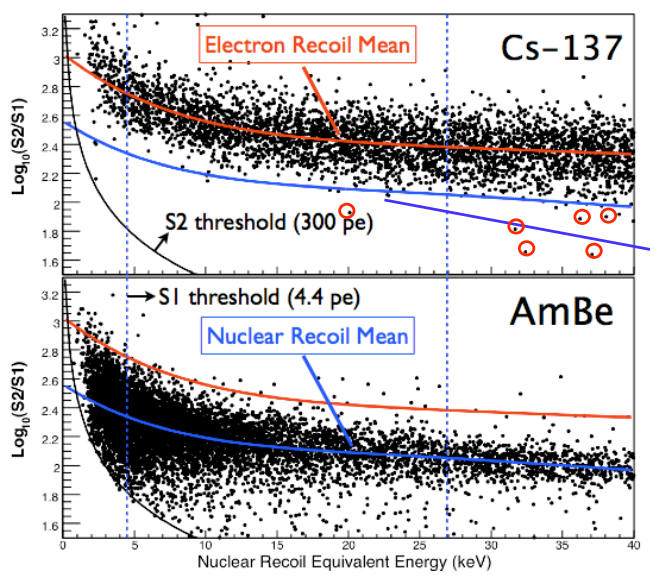

Figure 14: Calibration of the XENON10 detector using electron-recoil and neutron-recoil data. The region between the vertical dashed lines is the energy window (4.5 – 26.9 keVr) chosen for the WIMP search 99.5% of gamma events are rejected below the nuclear recoil mean. Image from [114].

Cuts based on energy and fiducial cuts are software-level and are performed after data is recorded to tape. This is what makes low-rate experiments so different from particle colliders: there's no need for a trigger to throw out any events.

5.5 XENON10

We now review the results of the XENON10 experiment. For simplicity[14] we shall focus on the spin-independent results presented in [112]. Just for fun we include a schematic of the XENON10 apparatus in Fig. 15.

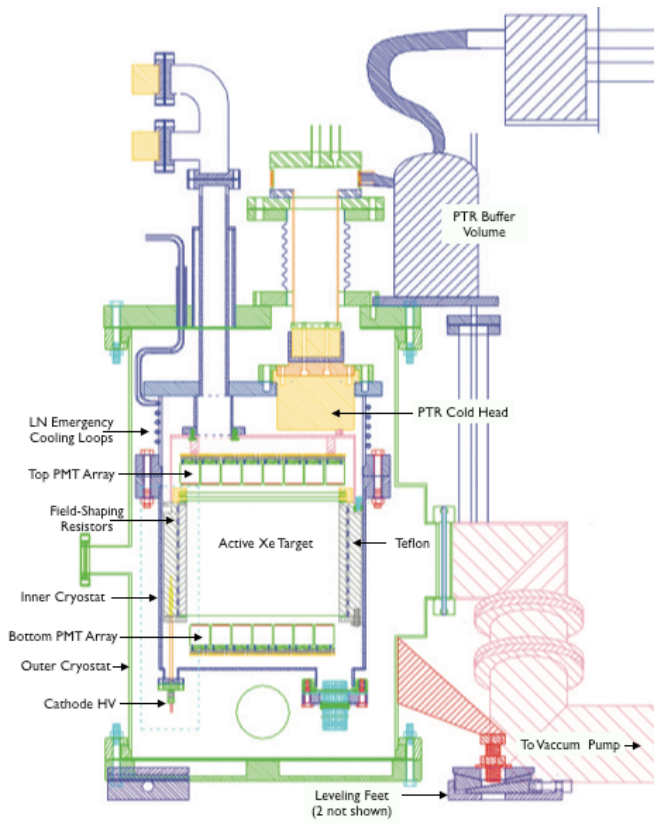

Figure 15: A schematic of the XENON10 apparatus. Image from K. Giboni in [116].

The limits set by XENON10 are presented below in Fig. 19. For the most part this is the 'bottom line.' However, let's instead discuss some features of the collaboration's data analysis.

XENON10 collected 58.6 live days of WIMP-search data. Out of a total of ∼1800 events, ten events survived the cuts. These are presented on a $\Delta\log(S_2/S_1)$ plot in Fig. 16 and on a 3D position plot in Fig. 17.

The question to ask is how many of these events are actually likely to be WIMP scatters. The XENON10 estimate for the expected number of anomalous 'leakage' events is limited by calibration statistics. Based on multiple-scatter calibration data, no neutron induced recoils are expected among the post-cut events.

[14] And because the author is desperately running out of time for this exam...

Before going into a post-cut analysis of these events, the collaboration set conservative upper bounds on the WIMP-nucleon cross section (see Fig. 19). The largest source of systematic uncertainty came from limited knowledge of the nuclear recoil scintillation efficiency at low recoil energies since measurements of this quantity were all above 10.8 keVr. At this limit the systematic uncertainty is 13.0 ± 2.4 %.

None of the 10 WIMP-candidate events are likely to be actual WIMP-interactions. Five of the events (numbers 3,4,5,7,9 in the figures) are statistically consistent with the electron recoil band. Further, it was found that event 1 met the coincidence requirement only because of a noise glitch. The remaining events (2,6,8,10) are not favored for three reasons:

1. They are clustered in the lower part of the fiducial volume (Fig. 17) where anomalous events (e.g. multiple scatters) occur more frequently.

2. An independent blind analysis performed in parallel to the primary analysis used more stringent $S1$ hit pattern cuts and rejected events 6,8, and 10.

3. The expected nuclear recoil spectrum prefers lower-energy scattering while these candidate events appear preferentially at higher energy (where we expect form factor suppression to reduce the WIMP signal).

5 events consistent with tail of gammas. A few that were mis-reconsutrcted, (double scatter).

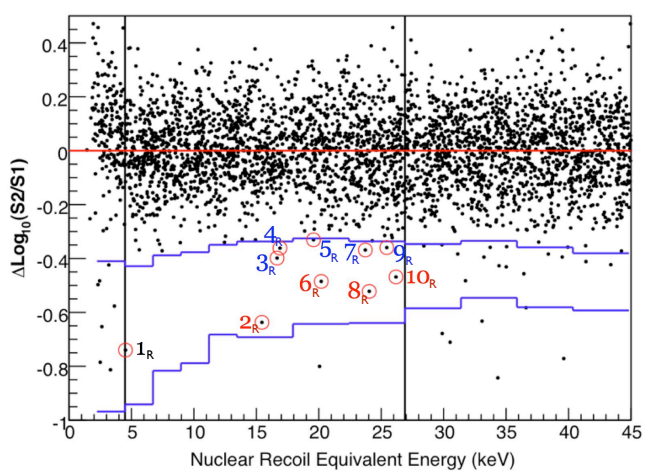

Figure 16: Ten candidate events from XENON10 plotted according to S_2/S_1. Blue lines and vertical lines show the WIMP-search region. Candidate events are numbered. Blue events are statistically consistent with electron recoil. Image from [116] based on results from [112].

6 Anticipating XENON 100

Let us now move on to a rather subjective and somewhat speculative[15] discussion of where we stand in anticipation of XENON100.

[15]Some of the discussion below was brought to the author's attention via the blogosphere [117], i.e. the 'yellow journalism' of physics.

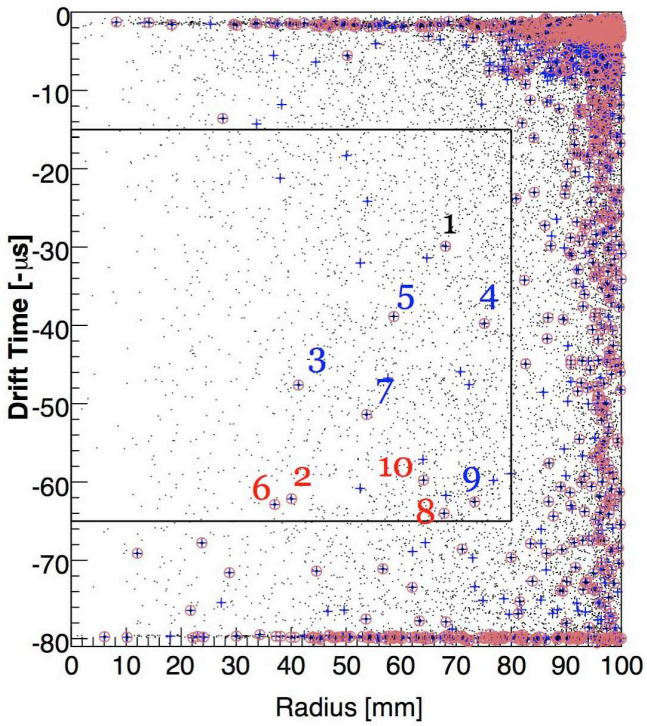

Figure 17: Ten candidate events from XENON10 plotted according to 3D position in the detector. The box shows the fiducial cut. Candidate events are numbered. Red events are in a region with higher probability for multiple scattering background. Image from [112].

6.1 Reach of the XENON100 experiment

Recent presentations from the XENON collaboration have suggested very impressive background rejection [114]. Fig. 18 shows preliminary data to compare with the XENON10 results. After fiducializing the larger detector volume ($\sim$ 40 kg fiducial volume) and imposing energy cuts, the preliminary data show *zero* background events. This data came from a short 11 day run and is already competitive with multi-month CDMS runs. The data set to be released this summer is expected to be ten times larger and the analysis will be bolstered with better measurements of the LXe scintillation efficiency at low recoil energies.

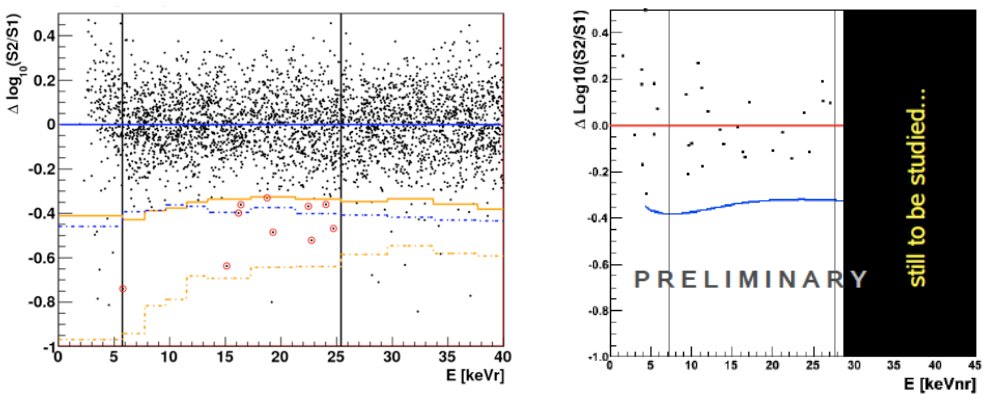

Figure 18: Left: XENON 10 events for 136 kg-days of exposure [112] showing candidate events in the nuclear recoil region. (In Section 5.5 we discuss the unblind analysis that removed these events.) Right: preliminary data from XENON100 with 190.4 kg-days of exposure [114].

6.2 What did CDMS see?

Probably nothing. (I'm supposed to say that or else my adviser will worry that he's been raising a crackpot.) At the end of 2009, the unblinding of 194 additional kg-days lead to the observation of two low-energy WIMP candidate events with 0.8 ± 0.3 background events expected [69]. Even with these background events, CDMS II had set the most sensitive bounds for direct detection with a representative exclusion point of 3.8×10^{-1}pb for $m_\chi = 70$ GeV.

The unfinished part of this story is the yet-to-be-announced results from the CDMS silicon detectors. Silicon is a light element ($A = 28$) and is important for light WIMP candidates. Speaking of light dark matter...

6.3 CoGeNT, DAMA, CRESST

Part of the 'sales pitch' from the XENON collaboration is their ability to test the infamous DAMA signal. Both NaI and Xe are excellent scintillators with similar energy thresholds (they are neighbors on the periodic table). Unlike DAMA, however, the XENON has 'automatic' background reduction from self-shielding and fiducialization (is this even a word?). XENON100 should be able to set comparable spin-dependent cross section limits, see Fig. 20. XENON expects to have a background rate that is 100 times lower than DAMA/LIBRA [114].

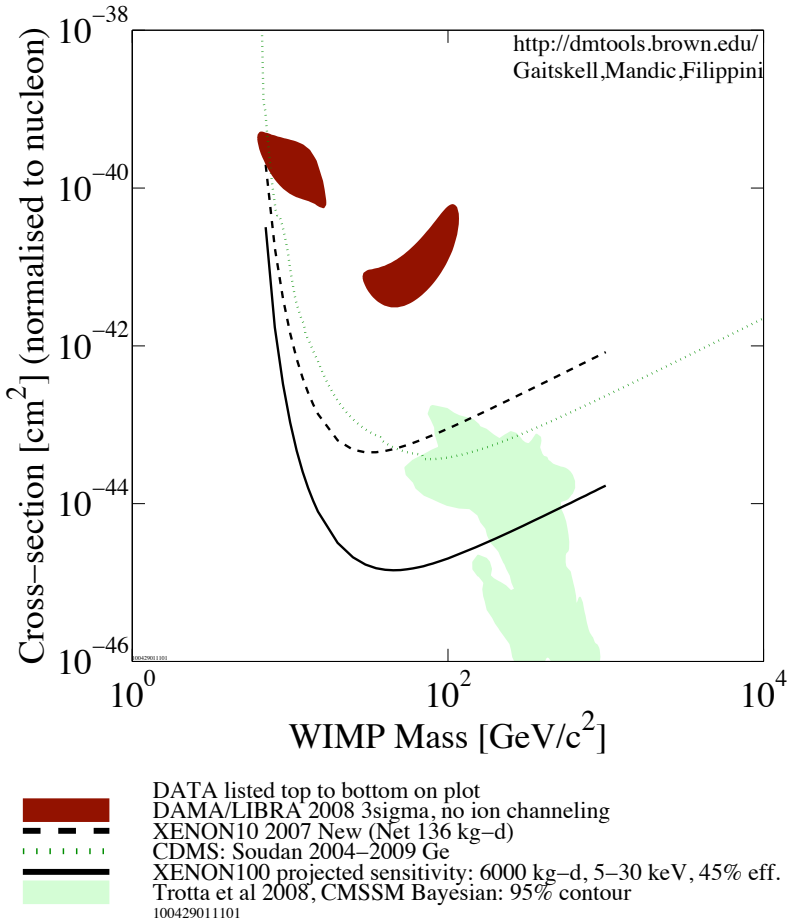

Figure 19: Spin-independent reach for XENON100 plotted against existing CDMS II bounds. Also shown are the DAMA region (no channeling) and an arbitrary slice of SUSY parameter space called the CMSSM. These regions should be taken with *mountains* of salt and are only provided to give a sense of XENON100's reach. Image generated by the author using [118].

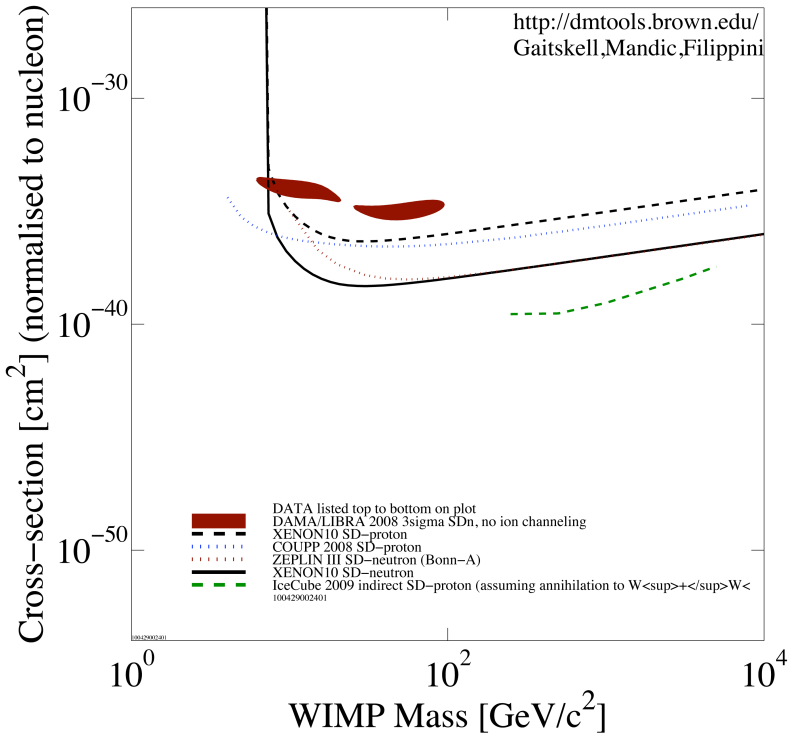

Figure 20: Spin-dependent constraints from XENON10 plotted against the DAMA region (no channeling) and related experiments. Image generated by the author using [118].

DAMA picked up some marginal interest earlier this year following anomalous events from the CoGeNT experiment [100]. Theorists noted that channeling and blocking phenomena could be used to shift around the DAMA and CoGeNT likelihood regions around so that they could approach one another [101].

The status of the DAMA and CoGeNT 'signals' are still the subject of current debate. For a fairly recent review about whether DAMA is compatible with other experiments, see [96]. Unfortunately at one year old this paper is already out-of-date. For recent rumor mongering one can refer to the usual suspects [117]. For a dose of sobering reality, see [6] for a discussion of non-dark matter sources for DAMA's annual modulation signal.

The bottom line is that XENON100 is a well-controlled experiment that plans to continue running through the rest of the calendar year to obtain a full dataset to search for any annual modulation signal. The similarities of xenon with iodine and the experiments' similar sensitivities should allow XENON to make meaningful exclusions on the DAMA 'parameter space.'

6.4 Hints from Pamela/FERMI

If you are doing everything well, you are not doing enough.
– Howard Georgi, personal motto [109]

Out of self-respect I have nothing to say about this. Absolutely nothing.

6.5 Role of the LHC

Before I say anything, you already know what the take-home message is: complementary searches for dark matter are important. Any meaningful handle on dark matter will come from a combination of direct detection, direct production, and indirect detection. A nice heuristic plot of this is presented in Fig. 21.

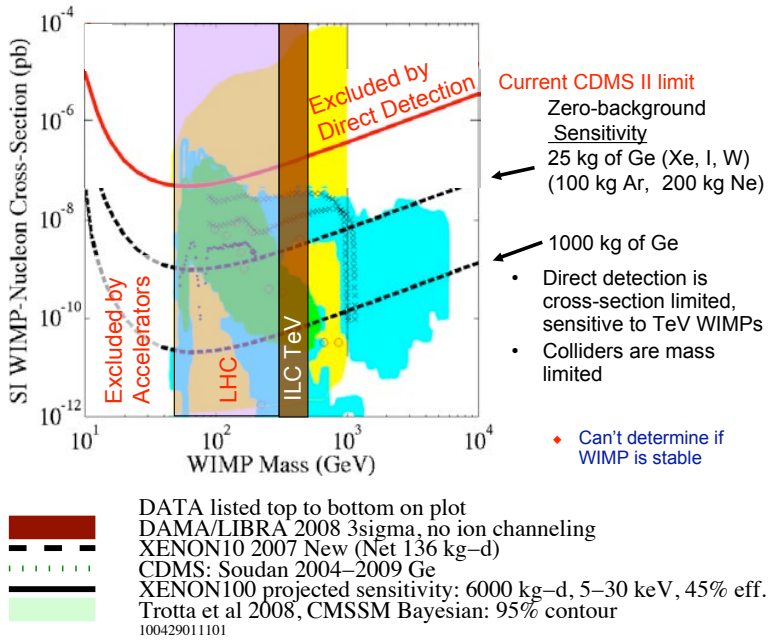

Figure 21: A heuristic plot of the complementary searches for dark matter. Image from [6].

Instead of saying anything meaningful about the role of the LHC, let us be somewhat defeatist and acknowledge that model-dependence makes it incredibly difficult to say anything meaningful about dark matter at the LHC. Every plot showing various 'preferred' SUSY regions should be viewed with skepticism (if not disdain), such regions should only be taken as *possible* points in parameter space and certainly not boundaries of parameter space in any sense. As we have seen above, there are enough model-building tricks to devise dark matter candidates that are arbitrarily hard to find at the LHC.

The difficulty at the LHC comes from the fact that dark matter will only show up as missing energy. It is premature to say anything about the plausibility of measuring dark matter couplings, but there has been some recent progress towards determining particle spectra in a model-independent way using so-called MT2 techniques[16]. The state-of-the-art for these techniques is subsystem MT2 and appears to hold some promise in determining invisible and intermediate particle spectra with sufficient luminosity [119].

[16]For a set of introductory notes on MT2 written by the author, see `http://www.lepp.cornell.edu/~pt267/files/BSMclub/Flip_09Oct26_notes.pdf`.

7 Outlook

The material here is a combination of a literature review, experimental preview, and 'how-to-interpret' guide for the XENON100 experiment (though most of our discussion is not specific to XENON). We have strived to present a document that can serve as a guidebook for phenomenologists who are considering the dark matter bandwagon. The extent to which we have been able to do this has been naturally limited by time constraints, but we hope to have provided sufficient references that the interested reader may continue where we have left off.

Further, this fall the Cornell BSM Journal Club[17] will host a student workshop on dark matter phenomenology. The author hopes that these notes can be expanded during that workshop.

There are many topics which we have unfortunately been unable to discuss. I highlight a few below, mostly for my own future reference.

- The role of neutrino telescopes on dark matter detection [120]
- The role of ground-based telescopes such as LSST
- The AMS experiment[18] which is a 'real' particle physics experiment in space (the spokesperson is Nobel prize winning particle experimentalist Sam Ting)
- The connection between dark matter and big bang nucleosynthesis [51]
- Gaseous detectors [121]
- Directional detectors
- Solar system dark matter, e.g. [122]

As we approach potentially exciting times in both dark matter and collider physics, it is important for phenomenologists to start considering the combination of a broad set of experimental programs to see how to extract meaningful model-independent information. A step towards this direction was taken in, e.g., [123].

Acknowledgements

I would like to thank the members of his A Exam committee: Csaba Csáki (chair), Liam McAllister, and Julia Thom (who proposed this question[19]).

Additionally, I thank Elena Aprile (spokesperson for the XENON collaboration), Evan Keane, and Bibhushan Shakya (who presented CoGeNT results at the Cornell BSM Journal Club) for useful discussions. Evan and Bibhushan also provided preliminary comments on Section 2 of this manuscript.

I would like to thank Neal Weiner and Richard Schnee for their lectures at TASI09[20].

[17] `http://www.lepp.cornell.edu/~pt267/journal.html`

[18] `http://www.ams02.org/`

[19] The final version of the prompt was prepared by the author, providing an manifestation of Kirk's solution to the Kobayashi-Maru test [124]. You win a prize if you appreciate the reference.

[20] I rescind any previously expressed sentiment that any of those lectures were 'boring' or 'sucked.'

I thank the "Emerging Problems in Particle Phenomenology" workshop sponsored by the ITS The Graduate Center (CUNY), the Starbucks on Seneca Street in Ithaca, the Cornell University Biological Field Station (located in Oneida, NY—a great place to hide from collaborators), and Waffle Frolic in downtown Ithaca for their hospitality during the completion of parts of this work.

Finally, many thanks to Liz Craig and Kasi Dean for keeping me alive during this examination.

This work is supported in part by the NSF grant number PHY-0355005, an NSF graduate research fellowship, and a Paul & Daisy Soros Fellowship For New Americans. The contents of this article do not necessarily represent the views of any of the aforementioned institutions or individuals.

A Notation and Conventions

WIMPs are generically referred to as χ. We use a subscript N to denote interactions with an entire nucleus and n for interactions with an individual nucle*on* I shouldn't even have to say it, but we work in natural units where $\hbar = c = 1$. Occasionally we will make factors of c explicit to make a point, but we will never write masses in GeV/c^2. Why do experimentalists keep doing that, anyway?

B Zero momentum transfer cross section

> Congratulations! If you're made it this far into the paper, then you've gotten to the stuff that I don't want to discuss during my oral exam.

Unfortunately, I didn't have time to flesh out the derivation of (3.9). The reader is forwarded to [106] and [125].

C Review of Dark Matter tools

In this appendix we survey some of the publicly available computer tools available for facilitating dark matter phenomenology. A recent review of available tools (focusing on SUSY) can be found in [126].

1. DM Tools [118] includes a very handy online interface for generating exclusion plots based on published data.

2. ILIAS DM Online Tools [127] is a set of complementary tools

3. Dark SUSY [53, 128] is a FORTRAN package for dark matter calculations in supersymmetry

4. micrOMEGAS [55, 54] is a particularly useful tool for properly integrating the Boltzmann equation in SUSY and select BSM models

D The WIMP miracle

This section to be written!

References

[1] **Particle Data Group** Collaboration, C. Amsler et al., "Review of particle physics," Phys. Lett. **B667** (2008) 1. A. Pierce, "Dark matter at the LHC,". In *Kane, Gordon (ed.) et al.: Perspectives on LHC physics* 13-23. D. Perkins, Particle Astrophysics (Oxford Master Series in Particle Physics, Astrophysics, and Cosmology). Oxford University Press, USA, 2003. E. Aprile and S. Profumo, "Focus on dark matter and particle physics," New J. Phys. **11** (2009) 105002.

[2] P. Burchat, "Patricia burchat sheds light on dark matter." `http://www.ted.com/talks/patricia_burchat_leads_a_search_for_dark_energy.html`. Talk at TEDGlobal 2005.

[3] G. Bertone, D. Hooper, and J. Silk, "Particle dark matter: Evidence, candidates and constraints," `hep-ph/0404175v2`. `http://arxiv.org/abs/hep-ph/0404175v2`. G. Bertone, ed., Particle dark matter: observations, models and searches. Cambridge University Press, 2010. Theoretical Advanced Study Institute In Elementary Particle Physics (TASI 2009, Physics Of The Large And The Small). SPIRES Conf Num: C09/06/01.3, 2009. `http://www.colorado.edu/physics/Web/tasi09_annc.html`. Recorded lectures available. See lectures by Neal Weiner and Richard Schnee.

[4] XXXV SLAC Summer Institute (SSI 2007), Dark Matter: from the Cosmos to the Laboratory. eConf C070730, SPIRES Conf Num: C07/07/30, 2007. `http://www-conf.slac.stanford.edu/ssi/2007/`.

[5] C.-L. Shan, "Extracting dark matter properties model-independently from direct detection experiments," `1003.0962v1`. `http://arxiv.org/abs/1003.0962v1`. C.-L. Shan, "Determining the Mass of Dark Matter Particles with Direct Detection Experiments," New J. Phys. **11** (2009) 105013, `arXiv:0903.4320 [hep-ph]`.

[6] Theoretical Advanced Study Institute In Elementary Particle Physics (TASI 2009, Physics Of The Large And The Small), Dark Matter Experiment. SPIRES Conf Num: C09/06/01.3, 2009. `http://www.colorado.edu/physics/Web/tasi09_annc.html`. See lectures by Richard Schnee, recordings available online.

[7] G. Chardin, "Dark matter direct detection," `astro-ph/0411503v3`. `http://arxiv.org/abs/astro-ph/0411503v3`. J. Gascon, "Direct search for wimp dark matter," `astro-ph/0504241v1`. `http://arxiv.org/abs/astro-ph/0504241v1`.

[8] R. J. Gaitskell, "Direct detection of dark matter," Ann. Rev. Nucl. Part. Sci. **54** (2004) 315–359.

[9] D. G. Cerdeno and A. M. Green, "Direct detection of wimps," 1002.1912v1. http://arxiv.org/abs/1002.1912v1.

[10] M. Roos, "Dark matter: The evidence from astronomy, astrophysics and cosmology," 1001.0316v1. http://arxiv.org/abs/1001.0316v1.

[11] E. Kolb and M. Turner, The Early Universe. Westview Press, 1994.

[12] P. D. Serpico and D. Hooper, "Gamma rays from Dark Matter Annihilation in the Central Region of the Galaxy," New J. Phys. **11** (2009) 105010, arXiv:0902.2539 [hep-ph]. M. Boezio et al., "PAMELA and indirect dark matter searches," New J. Phys. **11** (2009) 105023. A. Arvanitaki, S. Dimopoulos, S. Dubovsky, P. W. Graham, R. Harnik, and S. Rajendran, "Astrophysical probes of unification," 0812.2075v3. http://arxiv.org/abs/0812.2075v3.

[13] E. A. Baltz, M. Battaglia, M. E. Peskin, and T. Wizansky, "Determination of dark matter properties at high-energy colliders," hep-ph/0602187v4. http://arxiv.org/abs/hep-ph/0602187v4. J. L. Feng, "Collider Physics and Cosmology," Class. Quant. Grav. **25** (2008) 114003, arXiv:0801.1334 [gr-qc]. G. Kane and S. Watson, "Dark matter and lhc: What is the connection?," 0807.2244v1. http://arxiv.org/abs/0807.2244v1.

[14] H. Murayama, "Physics beyond the standard model and dark matter," 0704.2276v1. http://arxiv.org/abs/0704.2276v1. D. Hooper, "Tasi 2008 lectures on dark matter," 0901.4090v1. http://arxiv.org/abs/0901.4090v1.

[15] Theoretical Advanced Study Institute In Elementary Particle Physics (TASI 2009, Physics Of The Large And The Small), Dark Matter Theory. SPIRES Conf Num: C09/06/01.3, 2009. http://www.colorado.edu/physics/Web/tasi09_annc.html. See lectures by Neal Weiner, recordings available online.

[16] L. Bergstrom, "Dark matter candidates,".

[17] J. L. Feng, "Dark matter candidates from particle physics and methods of detection," 1003.0904v2. http://arxiv.org/abs/1003.0904v2.

[18] G. Jungman, M. Kamionkowski, and K. Griest, "Supersymmetric dark matter," hep-ph/9506380v1. http://arxiv.org/abs/hep-ph/9506380v1.

[19] "Dark matter portal: Experiments, conferences, tools." http://lpsc.in2p3.fr/mayet/dm.php. "Infn dark matter page." http://www.nu.to.infn.it/Dark_Matter/. "Net advance of physics: Dark matter." http://web.mit.edu/redingtn/www/netadv/Xdarkmatte.html.

[20] J. Einasto, "Dark matter," 0901.0632v1. http://arxiv.org/abs/0901.0632v1.

[21] XXXV SLAC Summer Institute (SSI 2007), Dark Matter: from the Cosmos to the Laboratory. eConf C070730, SPIRES Conf Num: C07/07/30, 2007. http://www-conf.slac.stanford.edu/ssi/2007/. See lectures by Leo Blitz, recordings available online.

[22] S. van den Bergh, "The Early History of Dark Matter," **111** (June, 1999) 657–660, arXiv:astro-ph/9904251.

[23] F. Zwicky, "Spectral displacement of extra galactic nebulae," Helv. Phys. Acta **6** (1933) 110–127.

[24] F. Zwicky, "Republication of: The redshift of extragalactic nebulae," General Relativity and Gravitation **41** (Jan., 2009) 207–224.

[25] S. Smith, "The Mass of the Virgo Cluster," **83** (Jan., 1936) 23–+.

[26] F. D. Kahn and L. Woltjer, "Intergalactic Matter and the Galaxy.," **130** (Nov., 1959) 705–+.

[27] "Fritz zwicky, scientist." http://www.mentalfloss.com/blogs/archives/1843#comment-2160.

[28] H. W. Babcock, "The rotation of the Andromeda Nebula," Lick Observatory Bulletin **19** (1939) 41–51.

[29] V. C. Rubin, "One hundred years of rotating galaxies," Publications of the Astronomical Society of the Pacific **112** (2000) no. 772, 747–750. http://www.journals.uchicago.edu/doi/abs/10.1086/316573.

[30] P. Giromini, F. Happacher, M. J. Kim, M. Kruse, K. Pitts, F. Ptohos, and S. Torre, "Phenomenological interpretation of the multi-muon events reported by the cdf collaboration," 0810.5730v1. http://arxiv.org/abs/0810.5730v1.

[31] J. P. Ostriker and P. J. E. Peebles, "A Numerical Study of the Stability of Flattened Galaxies: or, can Cold Galaxies Survive?," **186** (Dec., 1973) 467–480.

[32] D. Lynden-Bell, "Statistical mechanics of violent relaxation in stellar systems," **136** (1967) 101–+.

[33] J. P. Ostriker, P. J. E. Peebles, and A. Yahil, "The size and mass of galaxies, and the mass of the universe," **193** (Oct., 1974) L1–L4.

[34] 32nd SLAC Summer Institute on Particle Physics 32nd SLAC Summer Institute on Particle Physics: Nature's Greatest Puzzles. eConf C040802, SPIRES Conf Num: C04/08/02, 2007. http://www.slac.stanford.edu/econf/C040802/index.htm.

[35] B. Ryden, Introduction to Cosmology. Addison Wessley, 2003.

[36] C. Csaki, N. Kaloper, M. Peloso, and J. Terning, "Super-gzk photons from photon-axion mixing," hep-ph/0302030v2. http://arxiv.org/abs/hep-ph/0302030v2.

[37] K. M. Ashman, "Dark matter in galaxies," **104** (Dec., 1992) 1109–1138.

[38] K. Freese, "Review of observational evidence for dark matter in the universe and in upcoming searches for dark stars," 0812.4005v1. http://arxiv.org/abs/0812.4005v1. G. D'Amico, M. Kamionkowski, and K. Sigurdson, "Dark matter astrophysics," 0907.1912v1. http://arxiv.org/abs/0907.1912v1.

[39] D. Fabricant, M. Lecar, and P. Gorenstein, "X-ray measurements of the mass of M87," **241** (Oct., 1980) 552–560.

[40] R. Massey, T. Kitching, and J. Richard, "The dark matter of gravitational lensing," 1001.1739v1. http://arxiv.org/abs/1001.1739v1.

[41] D. Clowe, M. Bradac, A. H. Gonzalez, M. Markevitch, S. W. Randall, C. Jones, and D. Zaritsky, "A direct empirical proof of the existence of dark matter," astro-ph/0608407v1. http://arxiv.org/abs/astro-ph/0608407v1.

[42] S. Kachru, "Physics 153A: String Theory, Stanford University." Comment during lecture, 2006.

[43] S. Weinberg, Cosmology. Oxford University Press, USA, 2008.

[44] S. Sarkar, "Primordial nucleosynthesis and dark matter," astro-ph/9611232v1. http://arxiv.org/abs/astro-ph/9611232v1. K. A. Olive, "Primordial nucleosynthesis and dark matter," astro-ph/9707212v1. http://arxiv.org/abs/astro-ph/9707212v1.

[45] J. E. Carlstrom, G. P. Holder, and E. D. Reese, "Cosmology with the sunyaev-zel'dovich effect," astro-ph/0208192v1. http://arxiv.org/abs/astro-ph/0208192v1.

[46] D. H. Weinberg, R. Dav'e, N. Katz, and J. A. Kollmeier, "The lyman-alpha forest as a cosmological tool," astro-ph/0301186v1. http://arxiv.org/abs/astro-ph/0301186v1.

[47] E. L. Wright et al., "Preliminary spectral observations of the Galaxy with a 7 deg beam by the Cosmic Background Explorer (COBE)," Astrophys. J. **381** (1991) 200–209.

[48] N. Jarosik, C. L. Bennett, J. Dunkley, B. Gold, M. R. Greason, M. Halpern, R. S. Hill, G. Hinshaw, A. Kogut, E. Komatsu, D. Larson, M. Limon, S. S. Meyer, M. R. Nolta, N. Odegard, L. Page, K. M. Smith, D. N. Spergel, G. S. Tucker, J. L. Weiland, E. Wollack, and E. L. Wright, "Seven-year wilkinson microwave anisotropy probe (wmap) observations: Sky maps, systematic errors, and basic results," 1001.4744v1. http://arxiv.org/abs/1001.4744v1.

[49] W. Hu and S. Dodelson, "Cosmic microwave background anisotropies," astro-ph/0110414v1. http://arxiv.org/abs/astro-ph/0110414v1. W. Hu, N. Sugiyama, and J. Silk, "The physics of microwave background anisotropies," astro-ph/9604166v1. http://arxiv.org/abs/astro-ph/9604166v1.

[50] G. R. Blumenthal, S. M. Faber, J. R. Primack, and M. J. Rees, "Formation of galaxies and large-scale structure with cold dark matter," **311** (Oct., 1984) 517–525. J. R. Primack, "Dark matter and structure formation," arXiv:astro-ph/9707285.

[51] K. Jedamzik and M. Pospelov, "Big Bang Nucleosynthesis and Particle Dark Matter," New J. Phys. **11** (2009) 105028, arXiv:0906.2087 [hep-ph].

[52] P. Peebles, Principles of Physical Cosmology. Princeton University Press, 1993.

[53] P. Gondolo, J. Edsjo, P. Ullio, L. Bergstrom, M. Schelke, and E. Baltz, "Darksusy: Computing supersymmetric dark matter properties numerically," astro-ph/0406204v1. http://arxiv.org/abs/astro-ph/0406204v1.

[54] G. Belanger et al., "Indirect search for dark matter with micrOMEGAs2.4," arXiv:1004.1092 [hep-ph].

[55] "micromegas." http://lappweb.in2p3.fr/lapth/micromegas/.

[56] J. Hisano, K. Kohri, and M. M. Nojiri, "Neutralino warm dark matter," Phys. Lett. **B505** (2001) 169–176, arXiv:hep-ph/0011216. X.-l. Chen, M. Kamionkowski, and X.-m. Zhang, "Kinetic decoupling of neutralino dark matter," Phys. Rev. **D64** (2001) 021302, arXiv:astro-ph/0103452.

[57] L. A. Popa and A. Vasile, "Constraints on non-thermal Dark Matter from Planck lensing extraction," JCAP **0710** (2007) 017, arXiv:0708.2030 [astro-ph].

[58] F. Steffen, "Dark matter candidates - axions, neutralinos, gravitinos, and axinos,".

[59] J. L. Feng, "Dark matter at the fermi scale," astro-ph/0511043v1. http://arxiv.org/abs/astro-ph/0511043v1.

[60] F. Sánchez-Salcedo, E. Martínez-Gómez, and J. Magaña, "On the fraction of dark matter in charged massive particles (champs)," Journal of Cosmology and Astroparticle Physics **2010** (2010) no. 02, 031. http://stacks.iop.org/1475-7516/2010/i=02/a=031.

[61] S. Davidson, S. Hannestad, and G. Raffelt, "Updated bounds on milli-charged particles," JHEP **05** (2000) 003, arXiv:hep-ph/0001179.

[62] D. N. Spergel and P. J. Steinhardt, "Observational evidence for self-interacting cold dark matter," Phys. Rev. Lett. **84** (2000) 3760–3763, arXiv:astro-ph/9909386.

[63] L. Ackerman, M. R. Buckley, S. M. Carroll, and M. Kamionkowski, "Dark Matter and Dark Radiation," Phys. Rev. **D79** (2009) 023519, arXiv:0810.5126 [hep-ph].

[64] M. Kesden and M. Kamionkowski, "Galilean Equivalence for Galactic Dark Matter," Phys. Rev. Lett. **97** (2006) 131303, arXiv:astro-ph/0606566.

[65] M. Taoso, G. Bertone, and A. Masiero, "Dark Matter Candidates: A Ten-Point Test," JCAP **0803** (2008) 022, arXiv:0711.4996 [astro-ph].

[66] Wikipedia, "Baroque — wikipedia, the free encyclopedia," 2010. http://en.wikipedia.org/w/index.php?title=Baroque&oldid=355347171.

[67] "The dama project." http://people.roma2.infn.it/dama/. Collaboration website. **DAMA** Collaboration, R. Bernabei et al., "First results from DAMA/LIBRA and the combined results with DAMA/NaI," Eur. Phys. J. **C56** (2008) 333–355, arXiv:0804.2741 [astro-ph]. R. Bernabei et al., "Results from the DAMA/LIBRA experiment," J. Phys. Conf. Ser. **203** (2010) 012003.

[68] "The cdms homepage." http://cdms.berkeley.edu/.

[69] **CDMS II** Collaboration, "Dark Matter Search Results from the CDMS II Experiment,".

[70] S. R. Golwala, "Exclusion limits on the WIMP nucleon elastic scattering cross section from the Cryogenic Dark Matter Search,". UMI-99-94586.

[71] "Resonaances: What's really behind dama." http://resonaances.blogspot.com/2009/10/whats-really-behind-dama.html.

[72] J. Carr, G. Lamanna, and J. Lavalle, "Indirect detection of dark matter," Rept. Prog. Phys. **69** (2006) 2475–2512.

[73] M. Cirelli and A. Strumia, "Minimal Dark Matter predictions and the PAMELA positron excess," PoS **IDM2008** (2008) 089, arXiv:0808.3867 [astro-ph].

[74] "Pamela mission official website." http://pamela.roma2.infn.it.

[75] **HEAT** Collaboration, S. W. Barwick et al., "Measurements of the cosmic-ray positron fraction from 1- GeV to 50-GeV," Astrophys. J. **482** (1997) L191–L194, arXiv:astro-ph/9703192.

[76] **PAMELA** Collaboration, O. Adriani et al., "An anomalous positron abundance in cosmic rays with energies 1.5.100 GeV," Nature **458** (2009) 607–609, arXiv:0810.4995 [astro-ph].

[77] O. Adriani, G. C. Barbarino, G. A. Bazilevskaya, R. Bellotti, M. Boezio, E. A. Bogomolov, L. Bonechi, M. Bongi, V. Bonvicini, S. Bottai, A. Bruno, F. Cafagna, D. Campana, P. Carlson, M. Casolino, G. Castellini, M. P. D. Pascale, G. D. Rosa, D. Fedele, A. M. Galper, L. Grishantseva, P. Hofverberg, S. V. Koldashov, S. Y. Krutkov, A. N. Kvashnin, A. Leonov, V. Malvezzi, L. Marcelli, W. Menn, V. V. Mikhailov, M. Minori, E. Mocchiutti, M. Nagni, S. Orsi, G. Osteria, P. Papini, M. Pearce, P. Picozza, M. Ricci, S. B. Ricciarini, M. Simon, R. Sparvoli, P. Spillantini, Y. I. Stozhkov, E. Taddei, A. Vacchi, E. Vannuccini, G. Vasilyev, S. A. Voronov, Y. T. Yurkin, G. Zampa, N. Zampa, and V. G. Zverev, "A new measurement of the antiproton-to-proton flux ratio up to 100 gev in the cosmic radiation," 0810.4994v2. http://arxiv.org/abs/0810.4994v2.

[78] **LAT** Collaboration, W. B. Atwood et al., "The Large Area Telescope on the Fermi Gamma-ray Space Telescope Mission," Astrophys. J. **697** (2009) 1071–1102, arXiv:0902.1089 [astro-ph.IM]. A. A. Abdo, M. Ackermann, M. Ajello, W. B. Atwood, M. Axelsson, L. Baldini, J. Ballet, G. Barbiellini, D. Bastieri, M. Battelino, B. M. Baughman, K. Bechtol, R. Bellazzini, B. Berenji, R. D. Blandford, E. D. Bloom, G. Bogaert, E. Bonamente, A. W. Borgland, J. Bregeon, A. Brez, M. Brigida, P. Bruel, T. H. Burnett, G. A. Caliandro, R. A. Cameron, and P. A. Caraveo, "Measurement of the cosmic ray $e++e-$ spectrum from 20 gev to 1 tev with the fermi large area telescope,"Phys. Rev. Lett. **102** (May, 2009) 181101. K. M. Z. Bruce Winstein, "Cosmic light matter probes heavy dark matter,"Physics **2** (May, 2009) 37.

[79] N. J. Shaviv, E. Nakar, and T. Piran, "Natural explanation for the anomalous positron to electron ratio with supernova remnants as the sole cosmic ray source," Phys. Rev. Lett. **103** (2009) 111302, arXiv:0902.0376 [astro-ph.HE]. S. Profumo, "Dissecting Pamela (and ATIC) with Occam's Razor: existing, well-known Pulsars naturally account for the 'anomalous' Cosmic-Ray Electron and Positron Data," arXiv:0812.4457 [astro-ph].

[80] D. Finkbeiner, "Indirect Detection and Theoretical Models,"APS Meeting Abstracts (Feb., 2010) 1002–+.

[81] **H.E.S.S.** Collaboration, F. Aharonian et al., "HESS observations of the galactic center region and their possible dark matter interpretation," Phys. Rev. Lett. **97** (2006) 221102, arXiv:astro-ph/0610509. **HESS** Collaboration, F. Aharonian et al., "Search for Gamma-rays from Dark Matter annihilations around Intermediate Mass Black Holes with the H.E.S.S. experiment," Phys. Rev. **D78** (2008) 072008, arXiv:0806.2981 [astro-ph].

[82] C. Boehm, D. Hooper, J. Silk, M. Casse, and J. Paul, "MeV Dark Matter: Has It Been Detected?," Phys. Rev. Lett. **92** (2004) 101301, arXiv:astro-ph/0309686.

[83] W. de Boer, "Evidence for dark matter annihilation from galactic gamma rays?," New Astron. Rev. **49** (2005) 213–231, arXiv:hep-ph/0408166. W. de Boer, C. Sander, V. Zhukov, A. V. Gladyshev, and D. I. Kazakov, "Egret excess of diffuse galactic gamma rays as tracer of dark matter,"A&A **444** (dec, 2005) 51–67. http://dx.doi.org/10.1051/0004-6361:20053726. W. de Boer, C. Sander, V. Zhukov, A. V. Gladyshev, and D. I. Kazakov, "The supersymmetric interpretation of the EGRET excess of diffuse Galactic gamma rays," Phys. Lett. **B636** (2006) 13–19, arXiv:hep-ph/0511154.

[84] P. Mertsch and S. Sarkar, "Systematic effects in the extraction of the 'WMAP haze'," arXiv:1004.3056 [astro-ph.HE].

[85] G. Dobler, D. P. Finkbeiner, I. Cholis, T. R. Slatyer, and N. Weiner, "The Fermi Haze: A Gamma-Ray Counterpart to the Microwave Haze," arXiv:0910.4583 [astro-ph.HE].

[86] N. Weiner, "Beyond minimal dark matter." Talk at the ITS/CUNY Emerging Problems in Particle Phenomenology Workshop, 2010.

[87] A. Bottino, F. Donato, N. Fornengo, and S. Scopel, "Light neutralinos and WIMP direct searches," Phys. Rev. **D69** (2004) 037302, arXiv:hep-ph/0307303.

[88] D. Tucker-Smith and N. Weiner, "Inelastic dark matter," Phys. Rev. **D64** (2001) 043502, arXiv:hep-ph/0101138.

[89] D. Tucker-Smith and N. Weiner, "The status of inelastic dark matter," Phys. Rev. **D72** (2005) 063509, arXiv:hep-ph/0402065.

[90] I. Cholis, L. Goodenough, D. Hooper, M. Simet, and N. Weiner, "High Energy Positrons From Annihilating Dark Matter," Phys. Rev. **D80** (2009) 123511, arXiv:0809.1683 [hep-ph].

[91] P. W. Graham, R. Harnik, S. Rajendran, and P. Saraswat, "Exothermic Dark Matter," arXiv:1004.0937 [hep-ph].

[92] J. L. Feng, "Non-WIMP Candidates," arXiv:1002.3828 [hep-ph].

[93] J. L. Feng and J. Kumar, "The WIMPless Miracle: Dark-Matter Particles without Weak-Scale Masses or Weak Interactions," Phys. Rev. Lett. **101** (2008) 231301, arXiv:0803.4196 [hep-ph].

[94] L. D. Duffy and K. van Bibber, "Axions as Dark Matter Particles," New J. Phys. **11** (2009) 105008, arXiv:0904.3346 [hep-ph].

[95] N. Arkani-Hamed and N. Weiner, "LHC Signals for a SuperUnified Theory of Dark Matter," JHEP **12** (2008) 104, arXiv:0810.0714 [hep-ph].

[96] C. Savage, G. Gelmini, P. Gondolo, and K. Freese, "Compatibility of DAMA/LIBRA dark matter detection with other searches," JCAP **0904** (2009) 010, arXiv:0808.3607 [astro-ph].

[97] C. Savage, P. Gondolo, and K. Freese, "Can WIMP spin dependent couplings explain DAMA data, in light of null results from other experiments?," Phys. Rev. **D70** (2004) 123513, arXiv:astro-ph/0408346.

[98] D. S. Gemmell, "Channeling and related effects in the motion of charged particles through crystals," Rev. Mod. Phys. **46** (1974) 129–227.

[99] R. Bernabei et al., "Possible implications of the channeling effect in NaI(Tl) crystals," Eur. Phys. J. **C53** (2008) 205–213, arXiv:0710.0288 [astro-ph].

[100] R. Foot, "A CoGeNT confirmation of the DAMA signal," arXiv:1004.1424 [hep-ph].

[101] S. Chang, J. Liu, A. Pierce, N. Weiner, and I. Yavin, "CoGeNT Interpretations," arXiv:1004.0697 [hep-ph]. A. L. Fitzpatrick, D. Hooper, and K. M. Zurek, "Implications of CoGeNT and DAMA for Light WIMP Dark Matter," arXiv:1003.0014 [hep-ph].

[102] M. W. Goodman and E. Witten, "Detectability of certain dark-matter candidates," Phys. Rev. **D31** (1985) 3059.

[103] J. D. Lewin and P. F. Smith, "Review of mathematics, numerical factors, and corrections for dark matter experiments based on elastic nuclear recoil," Astropart. Phys. **6** (1996) 87–112.

[104] M. Kuhlen et al., "Dark Matter Direct Detection with Non-Maxwellian Velocity Structure," JCAP **1002** (2010) 030, `arXiv:0912.2358 [astro-ph.GA]`.

[105] C. S. Kochanek, "The Mass of the Milky Way galaxy," Astrophys. J. **457** (1996) 228, `arXiv:astro-ph/9505068`. M. Weber and W. de Boer, "Determination of the Local Dark Matter Density in our Galaxy," `arXiv:0910.4272 [astro-ph.CO]`.

[106] A. Kurylov and M. Kamionkowski, "Generalized analysis of weakly-interacting massive particle searches," Phys. Rev. **D69** (2004) 063503, `arXiv:hep-ph/0307185`.

[107] J. Engel, "Nuclear form-factors for the scattering of weakly interacting massive particles," Phys. Lett. **B264** (1991) 114–119.

[108] J. Engel, S. Pittel, and P. Vogel, "Nuclear physics of dark matter detection," Int. J. Mod. Phys. **E1** (1992) 1–37. J. Engel and P. Vogel, "Spin dependent cross-sections of weakly interacting massive particles on nuclei," Phys. Rev. **D40** (1989) 3132–3135. M. A. Nikolaev and H. V. Klapdor-Kleingrothaus, "Quenching of the spin-dependent scattering of weakly interacting massive particles on heavy nuclei,". Given at 3rd International Symposium on Weak and Electromagnetic Interactions in Nuclei (WEIN 92), Dubna, USSR, 16-22 Jun 1992.

[109] "Howard georgi's home page." `http://www.people.fas.harvard.edu/~hgeorgi/`.

[110] E. Armengaud, "Gif lectures on direct detection of dark matter," `1003.2380v1`. `http://arxiv.org/abs/1003.2380v1`.

[111] J. A. Formaggio and C. J. Martoff, "Backgrounds to sensitive experiments underground," Ann. Rev. Nucl. Part. Sci. **54** (2004) 361–412.

[112] **XENON** Collaboration, J. Angle et al., "First Results from the XENON10 Dark Matter Experiment at the Gran Sasso National Laboratory," Phys. Rev. Lett. **100** (2008) 021303, `arXiv:0706.0039 [astro-ph]`.

[113] J. Angle et al., "Limits on spin-dependent WIMP-nucleon cross-sections from the XENON10 experiment," Phys. Rev. Lett. **101** (2008) 091301, `arXiv:0805.2939 [astro-ph]`.

[114] "Xenon dark matter project: Presentations." `http://xenon.astro.columbia.edu/presentations.html`. See references to conferences on this page.

[115] E. Aprile and T. Doke, "Liquid xenon detectors for particle physics and astrophysics," 0910.4956v1. http://arxiv.org/abs/0910.4956v1.

[116] P. Sorensen, A Position-Sensitive Liquid Xenon Time-Projection Chamber for Direct Detection of Dark Matter: The XENON10 Experiment. PhD thesis, Brown University, 2008.

[117] "Resonaances: More trouble with dama." http://resonaances.blogspot.com/2010/04/more-trouble-with-dama.html. "Resonaances: More dark entries." http://resonaances.blogspot.com/2010/05/more-dark-entries.html.

[118] F. Gaitskell, Mandic, "Dark matter tools website." http://dmtools.brown.edu/.

[119] M. Burns, K. Kong, K. T. Matchev, and M. Park, "Using Subsystem MT2 for Complete Mass Determinations in Decay Chains with Missing Energy at Hadron Colliders," JHEP **03** (2009) 143, arXiv:0810.5576 [hep-ph].

[120] J. Liu, P.-f. Yin, and S.-h. Zhu, "Prospects for Detecting Neutrino Signals from Annihilating/Decaying Dark Matter to Account for the PAMELA and ATIC results," Phys. Rev. **D79** (2009) 063522, arXiv:0812.0964 [astro-ph]. F. Halzen and D. Hooper, "The Indirect Search for Dark Matter with IceCube," New J. Phys. **11** (2009) 105019, arXiv:0910.4513 [astro-ph.HE].

[121] G. Sciolla and C. J. Martoff, "Gaseous Dark Matter Detectors," New J. Phys. **11** (2009) 105018, arXiv:0905.3675 [astro-ph.IM].

[122] I. B. Khriplovich, "Capture of dark matter by the Solar System. Simple estimates," arXiv:1004.3171 [astro-ph.EP].

[123] P. Agrawal, Z. Chacko, C. Kilic, and R. K. Mishra, "Direct Detection Constraints on Dark Matter Event Rates in Neutrino Telescopes, and Collider Implications," arXiv:1003.5905 [hep-ph]. M. Beltran, D. Hooper, E. W. Kolb, and Z. C. Krusberg, "Deducing the nature of dark matter from direct and indirect detection experiments in the absence of collider signatures of new physics," Phys. Rev. **D80** (2009) 043509, arXiv:0808.3384 [hep-ph].

[124] W. contributors, "Kobayashi maru," 2010. http://en.wikipedia.org/w/index.php?title=Kobayashi_Maru. Page Version ID: 356235241.

[125] F. Giuliani, "Model-independent limits from spin-dependent wimp dark matter experiments," Phys. Rev. D; Physical Review D" **71** (2005) no. 12, .

[126] F. Boudjema, J. Edsjo, and P. Gondolo, "Susy tools for dark matter and at the colliders," 1003.4748v1. http://arxiv.org/abs/1003.4748v1.

[127] "Dark matter online tools." http://pisrv0.pit.physik.uni-tuebingen.de/darkmatter/.

[128] P. Gondolo, J. Edsjö, P. Ullio, L. Bergström, M. Schelke, E.A. Baltz, T. Bringmann and G. Duda, "DarkSUSY webpage." http://www.physto.se/~edsjo/darksusy. Nagoya University GCOE Winter School 2010: Dark Matter and Dark Energy. 2010. http://www.gcoe.phys.nagoya-u.ac.jp/dmde2010/lecturer.html. Notes available online.